

THESIS FOR THE DEGREE OF DOCTOR OF PHILOSOPHY

THE MULTIFUNCTIONAL PIPETTE
A MICROFLUIDIC TECHNOLOGY FOR THE BIOSCIENCES

ALAR AINLA



Department of Chemical and Biological Engineering
CHALMERS UNIVERSITY OF TECHNOLOGY

Göteborg, Sweden 2013

The Multifunctional Pipette
A Microfluidic Technology for the Biosciences
ALAR AINLA

ISBN: 978-91-7385-818-2

©Alar Ainla, 2013

Doktorsavhandlingar vid Chalmers tekniska högskola

Ny serie nr: 3499

ISSN: 0346-718X

Department of Chemical and Biological Engineering
Chalmers University of Technology
SE-412 96 Göteborg
Sweden
Telephone: +46-(0)31 772 1000

Front cover image: Multifunctional pipette -- a toolbox for single-cell and biomembrane studies. You may guess which tool represents which experiment in the papers!

Back cover photo by Viktoria Gusak

Printed by Chalmers reproservice
Göteborg, Sweden 2013

The Multifunctional Pipette

A Microfluidic Technology for the Biosciences

ALAR AINLA

Department of Chemical and Biological Engineering
Chalmers University of Technology

ABSTRACT

The theme of the work described in this thesis is the generation and application of liquid microenvironments in chemistry and bioscience using microfluidic devices. First, a computer controlled multi-stage dilution system to generate time-dependent chemical waves was developed, and its application was demonstrated on model biomembranes. Thereafter the focus was shifted towards spatial control of chemistry. Using a hydrodynamic flow confinement concept in an open liquid volume, we created a device coined “*Multifunctional Pipette*”. It features localized liquid handling at the single-cell size scale together with fast solution exchange. The technology has been refined and optimized to provide a feature-rich tool for biologists working with cells and tissues in microscopy experiments. Application examples include cell zeiosis, single-cell dose-response determination and ion-channel stimulation. Subsequent studies cover modifications and applications of this device, such as on-chip electrodes and electroporation, as well as uses in cell cultures, on tissue slices, and as an optofluidic thermometer. Finally, localized liquid handling has been applied to assemble 2-dimensional fluidic networks consisting of directly written supported lipid bilayers. This “*Lab on a Membrane*” toolbox allows rapid prototyping of 2D-fluidic circuits, to modify their chemistry and connectivity on-demand and to apply them in studies of molecular interactions.

Keywords: Microfluidics, microfabrication, PDMS, microfluidic dilution, microfluidic mixer, hydrodynamic flow confinement, microfluidic superfusion, single-cell analysis, supported lipid membranes, microfluidic temperature sensing.

LIST OF PUBLICATIONS

I A Microfluidic Diluter Based on Pulse Width Flow Modulation

Alar Ainla, Irep Gözen, Owe Orwar & Aldo Jesorka

Analytical Chemistry 2009, 81(13), 5549-5556.

II A Microfluidic Pipette for Single-Cell Pharmacology

Alar Ainla, Erik T. Jansson, Natalia Stepanyants, Owe Orwar & Aldo Jesorka

Analytical Chemistry, 2010, 82(11), 4529-4536.

III A multifunctional pipette

Alar Ainla, Gavin D. M. Jeffries, Ralf Brune, Owe Orwar & Aldo Jesorka

Lab on a Chip, 2012, 12(7), 1255-1261.

IV Single-Cell Electroporation Using a Multifunctional Pipette

Alar Ainla, Shijun Xu, Nicolas Sanchez, Gavin D. M. Jeffries & Aldo Jesorka

Lab on a Chip, 2012, 12(22), 4605-4609.

V A multifunctional pipette for localized drug administration to brain slices

Aikeremu Ahemaiti, Alar Ainla, Gavin D. M. Jeffries, Holger Wigström, Owe Orwar, Aldo Jesorka & Kent Jardemark

Manuscript

VI An optofluidic temperature probe

Ilona Węgrzyn, Alar Ainla, Gavin D. M. Jeffries & Aldo Jesorka

Submitted manuscript

VII Lab on a Membrane: a Toolbox for Reconfigurable 2D Fluidic Networks

Alar Ainla, Irep Gözen, Bodil Hakonen & Aldo Jesorka

Submitted manuscript

CONTRIBUTION REPORT

- I** Proposed concept for the diluter. Designed and fabricated microfluidic devices. Designed pneumatic and electronic control system and software. Performed calibration and testing. Analyzed data and developed models. Participated in lipid spreading experiments. Designed figures. Contributed to the writing of the paper.
- II** Proposed the pipette concept. Designed and fabricated all microfluidic devices. Designed control mechanism and software. Performed calibrations and testing. Performed finite element modeling. Analyzed data. Participated in all biological experiments. Designed figures. Contributed to the writing of the paper.
- III** Contributed to the design of the pipette shape and interfacing. Designed and characterized microfluidic circuitries. Participated in switching speed experiments. Performed calculations and developed models. Performed biological experiments. Wrote the paper.
- IV** Participated and supervised electrode development. Designed electrical interface. Participated in all biological experiments. Performed calculations and developed models. Designed figures. Contributed to the writing of the paper.
- V** Participated in intracellular recording experiments. Designed figures. Contributed to the writing of the paper.
- VI** Proposed concept of dye multiplexing. Developed models and performed simulations. Participated in experimental planning. Participated in all experiments. Contributed to data analysis. Designed figures. Contributed to the writing of the paper.
- VII** Proposed concepts of writing and erasing lipids using multifunctional pipette. Participated in experimental planning. Wrote control software. Participated in all experiments. Performed simulations. Analyzed and interpreted all data. Designed figures. Contributed to the writing of the paper.

PUBLICATIONS NOT INCLUDED IN THIS THESIS

Thermal Migration of Molecular Lipid Films as Contactless Fabrication Strategy for Lipid Nanotube Network

Irep Gozen, Mehrnaz Shaali, Alar Ainla, Bahanur Ortmen, Inga Pöldsalu, Kiryl Kustanovich, Gavin D. M. Jeffries, Paul Dommersnes, Zoran Konkoli & Aldo Jesorka

Submitted manuscript

Calibrated On-chip Dilution Module for the Multifunctional Pipette

Andreas Genner, Alar Ainla & Aldo Jesorka

Proceedings of the 3rd International Workshop on Soft Matter Physics & Complex Flows. Ed.: Jon Otto Fossum and Elisabeth Bouchaud. Lofoten, Norway

Influence of Temperature on Enzyme Activity in Single Cells

Shijun Xu, Alar Ainla, Gavin D. M. Jeffries, Kent Jardemark, Owe Orwar & Aldo Jesorka

Manuscript

Book chapter:

Hydrodynamically Confined Flow Devices

Alar Ainla, Gavin D. M. Jeffries & Aldo Jesorka

In book "Hydrodynamics - Theory and Model", by Jinhai Zheng, InTech, 2012

ISBN 978-953-51-0130-7

Review article:

Hydrodynamic Flow Confinement Technology in Microfluidic Perfusion Devices

Alar Ainla, Gavin D. M. Jeffries & Aldo Jesorka

Micromachines 2012, 3(2), 442-461.

RELATED PATENT APPLICATIONS

PIPETTES, METHODS OF USE, AND METHODS OF STIMULATING AN OBJECT OF INTEREST

Alar Ainla, Owe Orwar & Aldo Jesorka

PCT/IB2010/003307. Priority: Dec 3^d 2009.

MICROFLUIDIC DEVICE WITH HOLDING INTERFACE AND METHODS OF USE

Alar Ainla, Gavin D. M. Jeffries, Owe Orwar & Aldo Jesorka

PCT/US12/36758. Priority: May 6th, 2011.

METHOD OF HYDRODYNAMIC MANIPULATION OF OBJECTS ATTACHED TO A TWO-DIMENSIONAL FLUID

Alar Ainla, Bodil Hakonen, Irep Gözen, Owe Orwar & Aldo Jesorka

US Provisional Patent Application. Priority: July 30th, 2012.

METHOD TO FABRICATE, MODIFY, REMOVE AND UTILIZE FLUID MEMBRANES

Alar Ainla, Irep Gözen & Aldo Jesorka

US Provisional Patent Application. Priority: January 19th, 2013.

NOTATIONS & ABBREVIATIONS

ABBREVIATIONS

AFM	<i>Atomic force microscopy</i>
AMPA	<i>2-amino-3-(β-hydroxy-δ-methyl-isoxazol-4-yl) propanoic acid</i>
AOBS	<i>Acousto-optical beam splitter</i>
APD	<i>Avalanche photodiode</i>
APTES	<i>3-aminopropyl triethoxy silane</i>
CE	<i>Capillary electrophoresis</i>
CLSM	<i>Confocal laser scanning microscopy</i>
COC	<i>Cyclic olefin copolymer</i>
COP	<i>Cyclic olefin polymers</i>
DNA	<i>Deoxyribonucleic acid</i>
DPN	<i>Dip-pen nanolithography</i>
DQN	<i>Diazoquinone</i>
DRIE	<i>Deep reactive-ion etching</i>
FCS	<i>Fluorescence correlation spectroscopy</i>
FDP	<i>Fluorescein diphosphate</i>
FEM	<i>Finite element method</i>
FRAP	<i>Fluorescence recovery after photobleaching</i>
FRET	<i>Förster resonance energy transfer</i>
GABA	<i>γ-Aminobutyric acid</i>
GFP	<i>Green fluorescent protein</i>
HCF	<i>Hydrodynamically confined flow</i>
HF	<i>Hydrofluoric acid</i>
LTI	<i>Linear time invariant</i>
MEMS	<i>Microelectromechanical system</i>
NA	<i>Numerical aperture</i>
PC	<i>Polycarbonate</i>
PDE	<i>Partial differential equation</i>
PDMS	<i>poly(dimethylsiloxane)</i>
PMMA	<i>poly(methyl methacrylate)</i>
PMT	<i>Photomultiplier tube</i>
PWFM	<i>Pulse-width flow modulation</i>
PWM	<i>Pulse-width modulation</i>
SICM	<i>Scanning ion-conductance microscopy</i>
SOI	<i>Silicon on insulator</i>
TEOS	<i>Tetraethyl orthosilicate</i>
TIRF	<i>Total internal reflection fluorescence</i>
TPE	<i>Thermoplastic elastomer</i>
TRPV1	<i>Transient receptor potential vanilloid</i>

PHYSICAL NOTATIONS

Re *Reynolds number*

Pe *Peclet number*

St *Strouhal number*

p *Pressure*

Q *Flow rate*

R *Flow resistance*

G *Flow conductance*

C *Compliance*

c *Concentration*

MATHEMATICAL NOTATIONS

\oint_s *Integral over closed surface*

\iiint_v *Integral over volume*

\otimes *Convolution*

∇ *Nabla operator*

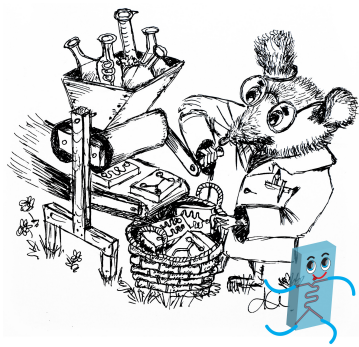
CONTENTS

1. Introduction	3
2. Fundamentals of Microfluidics	7
2.1 Fluid Physics	7
2.1.1 Flow.....	7
2.1.2 Mass Transport & Diffusion	13
2.1.3 Temperature	20
2.2 Microfluidics <i>versus</i> Microelectronics.....	21
2.2.1 Analogies.....	21
2.2.2 Circuits	23
2.2.3 Differences	26
3. Methods	29
3.1 Fabrication of Microfluidic Devices.....	29
3.1.1 Additive Techniques	31
3.1.2 Subtractive Techniques.....	31
3.1.3 Forming Techniques.....	33
3.1.4 Channel Sealing.....	35
3.1.5 Other Methods.....	36
3.1.6 Materials.....	36
3.1.7 Photolithography.....	38
3.1.8 PDMS Microfluidics	41
3.2 Microscopy.....	44
3.3 Simulations.....	49
4. Technology.....	51
4.1 Microfluidic Dilution	51

4.2 Localized Delivery of Chemicals	54
4.2.1 Hydrodynamic Flow Confinement	54
4.2.2 Solution Exchange - Need for Speed.....	59
4.2.3 Other Methods to Deliver Chemicals.....	61
4.3 Functional Biomembranes.....	62
4.3.1 Structure of the Biomembrane	62
4.3.2 Properties of the Biomembrane	63
4.3.3 Supported Lipid Membrane Technologies	63
Summary	65
Acknowledgements	69
References	71

Appendix

Papers I-VII



1. INTRODUCTION

Squeezing flasks and tubes from chemistry labs into small chips filled with networks of channels, valves, mixers and reaction chambers is a goal of the new and rapidly blooming field of Microfluidics. These so called 'Lab on a Chip' devices may eventually revolutionize medical diagnostics as well as chemical and biological analysis and research.

-- In the 23rd century, interplanetary travel has become as common as flights from London to Paris a few centuries ago. Of course, mankind hasn't made progress only in rocket science. A traveler has great need for protection, while wandering in the vastness of space. That's why Starfleet is equipped with Tricorders [1]- handheld devices which can help, while scouting on an alien planet or examining the health of a person, to detect infections by space bugs. -- With this vision of the future depicted in the 1960's cult series Star Trek, director Gene Roddenberry was mere decades ahead of his time. It was in the 1980s, when a microfabricated gas-chromatography column was actually putting forward the first steps towards miniaturization in chemical analysis [2]. And it took yet another decade, until in 1991, the Swedish company Pharmacia Biosensor AB (later Biacore AB, now part of GE Healthcare) coined the name 'Microfluidics' in one of their scientific papers [3]. Despite of this little known origin, the term 'Microfluidics' has now become synonymous with an entire field of science and technology, which is focusing on liquid manipulation and chemistry inside microscale devices. The field has exploded during the last decade, which is indicated by a doubling of the number of scientific publications and patent applications in less than every three years (Figure 1.1 A). Of course, such intensive research has resulted in a multitude of achievements, including deeper understanding of fluid physics at small scales, different means of fabrication and control, numerous applications and already more than a hundred companies making microfluidics-related products. Still, when looking at the typical technology lifecycle model (Figure 1.1 B), microfluidics is in its puberty, undergoing rapid development toward maturation [4], which includes improvements in manufacturing as well as identification of new applications. This shall pave the way for the wide-scale use of the technology, eventually bringing benefits for the society in general, such as faster, cheaper and more comprehensive diagnostics [5]. While the interplanetary spaceships from the Star Trek world are still a matter of science fiction, the medical Tricorder, helping to tackle "earth bugs", is actually almost within our reach. In 2012 Qualcomm was announcing a Tricorder X Prize of 10 million USD for the team to successfully build a portable device which is able to detect autonomously 15 distinct and common diseases, and does it better or at least as good as a trained physician [6]. This device would allow to keep better track of

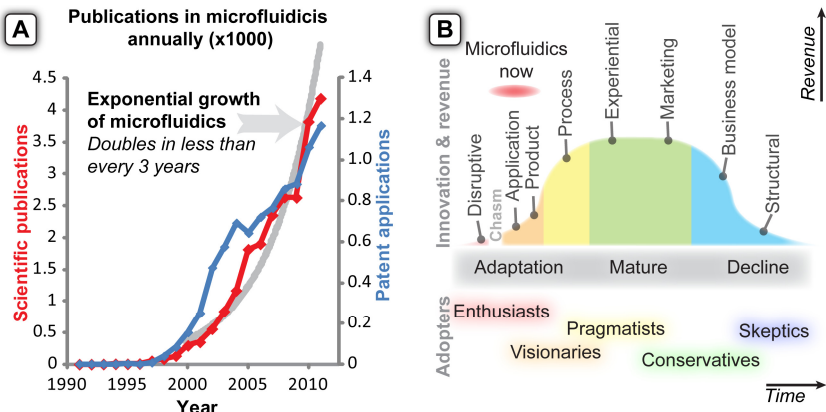


Figure 1.1. Development of microfluidics technology. (A) Growth of microfluidics during the last two decades. Based on scientific (ISI Web of Knowledge) and patent (espacenet) databases. (B) Microfluidics in the technology life cycle. Different phases of innovation, adaptation and economic impact [7-8].

personal health, prevent diseases, and reduce queues in front of doctors' doors. All of these points are of critical importance in the future, since the aging population will inevitably increase the social burden of healthcare needs.

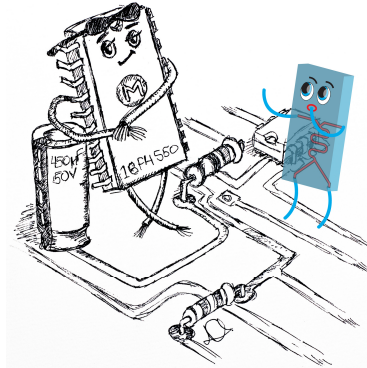
Microfluidics is not only holding promises in diagnostics, but can also extend the technical possibilities in our chemical, biological and medical research laboratories, for example by increasing efficiency and throughput, or by providing equipment in size scales specifically fitted to address single cells or their parts.

The backbone of this thesis is indeed the development of microfluidics based research tools and components, providing biophysicists and biologists with new means to control the chemical environment around single-cells. The PhD project started with a computer controlled, general purpose microfluidic dilution device, designed to generate chemical waves with desired parameters (Paper I). When it turned out to be cumbersome to apply this initial device in real biological experiments, it inspired the development of the next concept, which we termed a microfluidic pipette (Paper II). This device allowed localized delivery of solutions at the size scale of single cells in open volumes. The concept was reshaped for improved usability, turning it into a multifunctional tool for bioscience research (Paper III). We have explored diverse uses of the device for single cell electroporation (Paper IV), delivery of neurochemicals to brain slices (Paper V), and temperature measurement (Paper VI), and finally made a leap into new application areas and established a general method for the printing and manipulation of 2D nanofluidic circuits - a "lab on a membrane" (Paper VII).

The thesis provides background and context for the research described in the included papers. First relevant fluid physics and transport processes are discussed,

followed by practical instructions and considerations for designing microfluidic systems, and then the methods relevant for the thesis, such as microfabrication, imaging with different microscopy tools, and modeling are listed. The final chapter provides an in-depth overview, and comparison of the specific technologies studied and developed in this thesis, which are dilution, delivery of chemicals to adherent cells, and lipid membrane manipulations.

The author hopes that the thesis will not only earn him an advanced degree, but also provides some inspiration for new students who are starting to explore the field of microfluidics, as well as some useful hints and guidance to consider before designing chips. Unfortunately, the relevance of the thesis could potentially be short lived, due to the rapid development of the field. On the other hand, that is exactly what is making it so exciting to work with!



2. FUNDAMENTALS OF MICROFLUIDICS

Microfluidics and its big brother Microelectronics. Microelectronics has provided a plenitude of inspiration, and also tools for fabricating Microfluidics. Both have similarities even when it comes to physical laws. Yet why has Microfluidics not been able to repeat the glory of its older sibling? Why it has been so difficult to fully mimic electronic systems? These questions will be addressed in the following chapter, along with a brief exploration of the physical principles of microfluidics.

2.1 FLUID PHYSICS

2.1.1 FLOW

Transport of liquid in microscale channels is central for most microfluidic systems, including the ones described in this thesis. Therefore it is important to understand the basic driving forces, mechanisms and properties of microflows. The mechanical aspect of the flow, which is the motion of liquid, is described by classical mechanics and hydrodynamics. In order to derive such a flow equation, one can actually start from basic principles of mechanics known as Newton's laws, named after Sir Isaac Newton, who formulated them in his work *Philosophiae Naturalis Principia Mathematica* at 1687. Most important are his 2nd and 3rd law (Eq 2.1 and Eq 2.2) relating acceleration and force acting on a body, and defining the mutuality of interactions.

$$\vec{a} = \frac{\vec{F}}{m} \quad (2.1)$$

where \vec{F} is the force acting on a body, m is its mass and \vec{a} the acceleration caused by the force.

$$\vec{F}_2 = -\vec{F}_1 \quad (2.2)$$

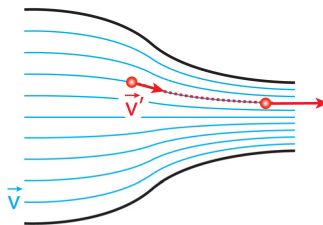


Figure 2.1. Steady flow in a tube with shrinking diameter. The concept of a velocity field \vec{v} (blue) and the velocity of a particular fluid particle \vec{v}' (red). Even though the velocity field is steady, the particular fluid particle can accelerate during its journey.

Which implies, that if one body affects another with force \vec{F}_1 , then the second body affects the first back with force \vec{F}_2 , which has the same magnitude, but acts in opposite direction.

While the original notion of Newton's 2nd law is well suited for describing falling apples and the motion of other solid objects, it is less convenient for handling liquid streams. For solid objects their coordinate and velocity is used to describe motion, while for fluids the **velocity field** becomes handier. It means that we are not looking at the velocity of one particular "fluid particle", but instead at the velocity of the fluid in a certain place in space. The important difference can be understood, if we imagine a constant flow rate in a tube, which means that the velocity field should be also constant. However, if the tube has a narrower region, the liquid needs to accelerate to pass it, since the flow velocity must be higher in the narrower region in order to maintain an overall constant flow rate. This means, that a particular fluid particle, which would always be a subject to Newton's 2nd equation, may experience acceleration, even if the velocity field is steady. This is illustrated in figure 2.1.

Lets express the acceleration of fluid particle \vec{a}' from the velocity field \vec{v} during an infinitely small time step dt . This acceleration would contain then two parts; one due to the change in the velocity field, and another due to the changing position of the particle in the steady field.

$$\vec{a}' = \frac{d\vec{v}'}{dt} = \underbrace{\frac{\vec{v}(t + dt) - \vec{v}(t)}{dt}}_{\text{temporal}} + \underbrace{\frac{\vec{v}(\vec{r}(t + dt)) - \vec{v}(\vec{r}(t))}{dt}}_{\text{spatial}} \quad (2.3)$$

Using the chain rule of differentiation on a spatial component, eq. 2.3 becomes

$$\vec{a}' = \frac{d\vec{v}(t)}{dt} + \underbrace{\frac{d\vec{r}(t)}{dt}}_{\vec{v}} \frac{d\vec{v}(\vec{r})}{d\vec{r}} \quad (2.4)$$

Since $\vec{v} = \vec{v}(t, \vec{r})$, the partial derivative notation shall be used here, giving

$$\vec{a}' = \frac{\partial \vec{v}(t, \vec{r})}{\partial t} + \vec{v} \frac{\partial \vec{v}(\vec{r})}{\partial \vec{r}} = \frac{\partial \vec{v}}{\partial t} + \vec{v} \cdot \nabla \vec{v} \quad (2.5)$$

From the acceleration of the fluid particle and its mass $d\mathbf{m}$, we calculate the force $d\vec{F}'$

$$d\vec{F}'_{net} = d\mathbf{m}\vec{a}' \quad (2.6)$$

In contrast to solid objects, the density ρ would be a more suitable descriptor of a fluid than the mass of some arbitrarily chosen particle:

$$d\vec{F}'_{net} = \rho dV \vec{a}' = \rho dV \left(\frac{\partial \vec{v}}{\partial t} + \vec{v} \cdot \nabla \vec{v} \right) \quad (2.7)$$

In most microfluidic systems where water solutions are used, it is safe to assume that the fluid is incompressible, which means that the density is a constant

$$\operatorname{div}(\vec{v}) = 0 \text{ and } \rho = const \quad (2.8)$$

As seen from eq. 2.7, even a steady flow of a liquid features acceleration, and therefore forces acting between the fluid particles. The most common forces, which are always present, are caused by pressure and the viscosity of the fluids.

Liquid pressure acts on all surfaces and exerts a force in perpendicular direction to them. In order to derive the force exerted to a liquid particle with volume V we need to integrate the pressure over the surface of this particle, where dS denotes a small surface element and \vec{n} points to its normal direction.

$$\vec{F}'_{pres.} = - \iint_{\text{surface of particle}} P \cdot \vec{n} dS \quad (2.9)$$

By using Ostrogratsky's divergence theorem, this integral over the surface can be turned into an integral over volume

$$\vec{F}'_{pres.} = - \iiint_{\text{volume of particle}} \nabla P dV \quad (2.10)$$

If the volume V is infinitely small, we will have a differential form of the equation

$$d\vec{F}'_{pres.} = -\nabla P dV \quad (2.11)$$

Where ∇P is the pressure gradient (also denoted $\operatorname{grad}(P)$)

Another important force is friction inside fluid flow, which happens when different parts of the liquid move at different velocity. This was also studied by Newton, who found that the force F required to overcome the friction and move two parallel plates

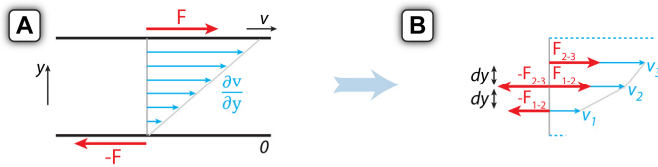


Figure 2.2. Viscosity. **(A)** Two parallel plates separated by a Newtonian fluid, moving relative to each other (also known as Couette flow). **(B)** Relating viscous forces and velocity field.

relative to each other, when both are separated by a fluid, is proportional to the velocity gradient (also called shear rate) $\partial v / \partial y$ and the area of the plates S (Figure 2.2A)

$$F = \eta S \frac{\partial v}{\partial y} \quad (2.12)$$

with a proportionality constant η , called **dynamic viscosity**, which is a characteristic property of the fluid, depending also on the temperature. However, this relation is correct only for some simple substances, called Newtonian fluids. In non-Newtonian fluids, like polymer solutions, η depends also on shear rate, making the behavior much more complex. Fortunately water and most dilute aqueous solutions used in microfluidics behave as Newtonian fluids, therefore we focus only on them.

Starting from Newton's law of viscosity we can derive how the viscous force inside the fluid is related to the velocity field. First let's imagine three close layers of fluid, which move with different speeds v_1 , v_2 and v_3 . If the layers are separated by distance dy , the forces acting between them can be calculated using Newton's viscosity law (2.12)

$$F_{2-3} = \eta S \frac{v_3 - v_2}{dy} \quad (2.13)$$

$$F_{1-2} = \eta S \frac{v_2 - v_1}{dy}$$

Taking into account Newton's 3rd law about the mutuality of interactions (Eq. 2.2) and summing forces from both sides, we can calculate the net force acting on the middle layer of the fluid

$$F = F_{1-2} - F_{2-3} = \eta S \left(\frac{v_2 - v_1}{dy} - \frac{v_3 - v_2}{dy} \right) \quad (2.14)$$

As seen from this equation the force acting on the fluid layer does not depend on the velocity gradient, but on its change, which can in case of infinitely small dy be described through the derivative of the gradient.

$$F = \eta S \frac{\partial}{\partial y} \left(\frac{\partial v}{\partial y} \right) dy = \eta \frac{\partial}{\partial y} \left(\frac{\partial v}{\partial y} \right) \underbrace{S dy}_{dV} \quad (2.15)$$

where dV is the volume of the layer. In order to generalize the equation, we calculate the force, considering infinitely small layers (dS) in three dimensions:

$$d\vec{F}'_{visc.} = \eta \nabla^2 \vec{v} dV \quad (2.16)$$

Now the different forces can be combined, and the net force is proportional to the acceleration

$$\begin{aligned} d\vec{F}'_{net} &= d\vec{F}'_{pres.} + d\vec{F}'_{visc.} \\ \rho dV \left(\frac{\partial \vec{v}}{\partial t} + \vec{v} \cdot \nabla \vec{v} \right) &= -\nabla P dV + \eta \nabla^2 \vec{v} dV \end{aligned} \quad (2.17)$$

After dividing both sides by dV we obtain the following differential equation

$$\rho \left(\frac{\partial \vec{v}}{\partial t} + \vec{v} \cdot \nabla \vec{v} \right) = -\nabla P + \eta \nabla^2 \vec{v} \quad (2.18)$$

This equation, named after 19th century French and British scientists Claude-Louis Navier and Sir George Gabriel Stokes (**Navier-Stokes' equation**) relates the velocity field of the flow with the pressure distribution and viscosity. It is a central concept in all flow calculations. Unfortunately, this non-linear partial differential equation is almost never analytically solvable. In fact, understanding Navier-Stokes' equation is considered one of the greatest unsolved problems in mathematics, with a million dollar prize promised to anyone who can elucidate its properties [9].

But some qualitative insight into the flow behavior and its dependence on the size scales can be obtained by using scaling laws. For that purpose eq. 2.18 can be re-written in a dimensionless form, using the following replacements

$$\tilde{r} = L_0 \vec{r}, \nabla = \frac{1}{L_0} \tilde{\nabla}, \tilde{v} = v_0 \vec{v}, t = \frac{L_0}{v_0} \tilde{t} \text{ and } P = \frac{\eta v_0}{L_0} \tilde{P} \quad (2.19)$$

Where \sim denotes dimensionless analogues. L_0 and v_0 are characteristic size and velocity scales.

$$\rho \left(\frac{v_0 \partial \tilde{v}}{L_0 \partial \tilde{t}} + v_0 \tilde{v} \cdot \left(\frac{v_0}{L_0} \right) \tilde{\nabla} \tilde{v} \right) = - \left(\frac{\eta v_0}{L_0^2} \right) \tilde{\nabla} \tilde{P} + \eta \left(\frac{v_0}{L_0^2} \right) \tilde{\nabla}^2 \tilde{v} \quad (2.20)$$

Re-arrangements lead to (eq. 2.21)

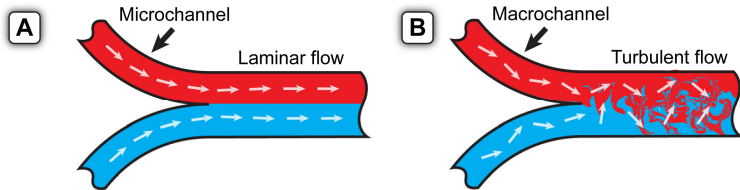


Figure 2.3. Velocity field. **(A)** Laminar flow. **(B)** Turbulent flow

$$\underbrace{\frac{\rho v_0 L_0}{\eta}}_{Re} \left(\frac{\partial \vec{v}}{\partial t} + \vec{v} \cdot \nabla \vec{v} \right) = -\nabla \tilde{P} + \tilde{\nabla}^2 \vec{v} \quad (2.21)$$

demonstrating that the dimensionless Navier-Stoke' equation depends only on one scaling parameter, known as **Reynolds number** (Re)

$$Re = \frac{\rho v_0 L_0}{\eta} \quad (2.22)$$

If Re is large ($Re \gg 1$), the equation is dominated by the left side, which describes inertia. Due to the non-linear term $\vec{v} \cdot \tilde{\nabla} \vec{v}$ the behavior of flow in a "high Reynolds number mode" is chaotic (**turbulent flow**). Alternatively, if Re is low ($Re \ll 1$), the inertial side can be neglected and the equation is dominated by pressure and viscosity terms. This linear equation, known as **Stokes' equation** (Eq 2.23) has a well defined solution, which corresponds to the **laminar flow** regime. In typical microfluidic systems, where the channel sizes are small and the flow is slow, the Reynolds number is low and the flow is laminar.

$$\nabla P = \eta \nabla^2 \vec{v} \quad (2.23)$$

Stokes' equation has analytical solutions for a variety of simple geometries like cylindrical and rectangular tubes. Due to fabrication constraints, microfluidic channels have most commonly rectangular geometry. In a long rectangular channel the flow field is [10]

$$v_x(y, z) = \frac{4h^2 \Delta p}{\pi^3 \eta L} \sum_{n, odd}^{\infty} \frac{1}{n^3} \left[1 - \frac{\cosh(n\pi \frac{y}{h})}{\cosh(n\pi \frac{w}{2h})} \right] \sin(n\pi \frac{z}{h}) \quad (2.24)$$

$$v_y = v_z = 0$$

Where L is the channel length along the x axis, h is the channel height along the z axis, w is the channel width along the y axis and Δp is the pressure difference between

the channel ends. If the velocity is integrated over the cross section, the total flow rate can be found as

$$\begin{aligned} Q &= \int_0^h \int_{-w/2}^{w/2} v_x(y, z) dy dz \\ &= \frac{h^3 w \Delta p}{12 \eta L} \left[1 - \sum_{n, odd}^{\infty} \frac{1}{n^5} \frac{192}{\pi^5} \frac{h}{w} \tanh \left(n\pi \frac{w}{2h} \right) \right] \end{aligned} \quad (2.25)$$

For practical purposes, this infinite series is still hard to calculate, therefore an approximation can be used

$$Q = \Delta p \frac{h^3 w}{12 \eta L} \left[1 - 0.630 \frac{h}{w} \right] \quad (2.26)$$

where $h < w$. In worst case, when the channel has a square cross-section, the error generated by using this approximation is actually only 13%.

2.1.2 MASS TRANSPORT & DIFFUSION

From a chemical point of view, it would be boring to pump just water. Therefore, most of the microfluidic systems handle a variety of solutions and regents, are able to mix and switch between them, and carry out chemical reactions. This introduces a new dimension into the equations – the chemical composition. In case there is no reactivity between different fluids and no strong interaction between composition and flow, the composition can be split into independent concentrations of molecules and each of them can be considered separately. An example for a case where composition and flow behavior are not independent would be sugar solution and water, where the sugar concentration determines viscosity and therefore flow, which would then again influence concentration. This type of coupling makes calculations significantly more complex. In contrast, the research presented in this thesis involved only dilute solutions, where the chemical composition has no major effect on the flow properties. In this case the concentration of a substance can be described by the **convection-diffusion equation** (Eq. 2.27)

$$\frac{\partial c}{\partial t} = -\vec{v} \cdot \nabla c + D \nabla^2 c \quad (2.27)$$

where the left-hand side describes the temporal change of the concentration, which depends on the convective transport by the flow ($-\vec{v} \cdot \nabla c$), and on diffusion ($D \nabla^2 c$). This equation has a striking similarity to the Navier-Stokes equation, where just c has been replaced by \vec{v} . Therefore, the Navier-Stokes equation can be considered as the transport equation of momentum, where viscosity acts as diffusivity of momentum.

If we convert the convection-diffusion equation into a dimensionless form, as we did previously with Navier-Stokes (Eq. 2.21), the resulting equation depends on two scaling parameters St and Pe

$$St \frac{\partial \tilde{c}}{\partial \tilde{t}} = -\vec{v} \cdot \tilde{\nabla} \tilde{c} + \frac{1}{Pe} \tilde{\nabla}^2 \tilde{c} \quad (2.28)$$

where St stands for the Strouhal number, describing unsteadiness, and Pe for **Peclet number**, describing the ratio between convective and diffusive mass transport. Pe is analogous to the Reynolds number, which describes the same for momentum.

$$St = \frac{L_0}{\tau v_0} \quad \text{and} \quad Pe = \frac{v_0 L_0}{D} \quad (2.29)$$

where τ is the unsteady time.

In the following we consider two important cases, which are both also relevant for the research presented in this thesis. First, a steady flow and concentration patterns, where $St = 0$, and second, transient propagation of concentration pulses in a pressure driven flow.

Steady flow

Our macro-world experience tells us that putting together two miscible liquids, for example syrup and water, will eventually result in their complete mixing. Microfluidics, on the other hand, offers an easy way to form and even maintain spatially constant concentration gradients. This requires that diffusion, which always mixes substances until the differences have faded, is compensated by the convective flow, which replaces mixed liquids. The dimensionless convection-diffusion equation (Eq. 2.28) shows that the stationary equation ($St=0$) depends on only one parameter, which is the Peclet number. Here, a higher Peclet number implies dominance of convection over diffusion, therefore less mixing and sharper concentration gradients, and vice versa. This is illustrated in figure 2.4, showing a typical T- or Y-channel, where two solutions enter a common channel, co-flow, and mix diffusively. The further we go from the junction point, the more diffusion has progressed, and the smoother is the gradient. A detailed description of the concentration profile is complex and requires numerical simulations. However, if we can assume a 2-dimensional channel with constant velocity, an analytical solution is possible (Eq. 2.30)

$$c(x, w, t/T_0) = \frac{c_0}{2} \sum_{n \in \pm \mathbb{N}} \left(\operatorname{erf} \left(\frac{x/w - (2n+1)}{\sqrt{t/T_0}} \right) - \operatorname{erf} \left(\frac{x/w - 2n}{\sqrt{t/T_0}} \right) \right) \quad (2.30)$$

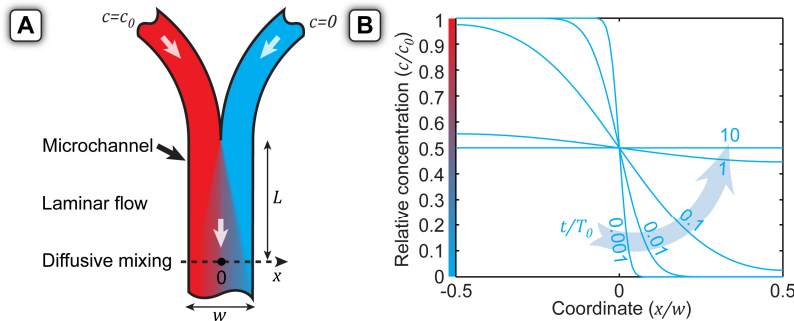


Figure 2.4. Stationary concentration gradients in microchannels. **(A)** A Y-shaped channel, fed by two flows, where one is carrying a solution of a substance with concentration c_0 , and the other one is pure solvent ($c=0$). Due to the lack of turbulence, these two flows mix only due to molecular diffusion, which smoothens the concentration difference between the flows. On the other hand this diffusive mixing is compensated by a replenishing supply of liquids. The balance between diffusion and convective replacement is establishing a stationary concentration distribution **(B)**. The concentration profile in this kind of channel depends only on one dimensionless time ratio t/T_0 . The greater the ratio, the smoother is the gradient.

where $T_0 = w^2/4D$ is characteristic time-scale of the system, and $t = L/v_{aver}$ is the time, during which diffusion has occurred. In reality this assumption is well suitable for high aspect ratio channels.

This principle has been used in a variety of devices, for example to generate concentration gradients for cell migration studies [11]. There is a class of separation techniques, based on devices called H-filters, where these two flows are split apart again at the end of the common channel [12]. The separation of the substances is based on their different diffusion properties. Even more efficient separation is achieved when active transport can be included and the selected substance can be dragged to one edge of the channel, for example by magnetic force [13], which has been used to remove pathogens from blood. The transport mode can be even biological. For example, similar filters have been used to separate live and dead sperms to improve *in vitro* fertilization [14]. Besides separation, this kind of dispersion in microchannels has to be considered when designing microfluidic mixers, to make sure that two fluids have become well blended at the end of a mixing channel.

The same principle of convection competing with diffusion has found an application in hydrodynamic flow confinement (HCF), allowing localized delivery of chemicals. HCF is a key element of the multifunctional pipette, studied in this thesis.

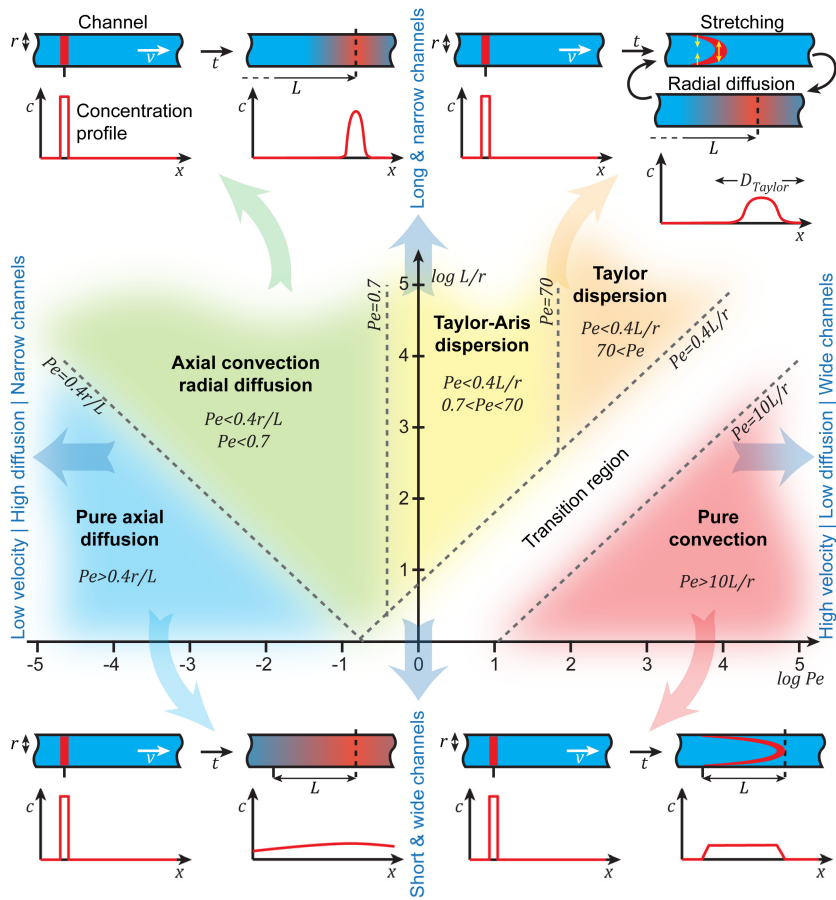


Figure 2.5. Dispersion models and their regions of applicability depending on Pe number and channel geometries (L/r). (According to Probstein "Physiochemical Hydrodynamics" [15]). The colors used to shade the regions have blurry edges to emphasize that the transitions between these modes are not sharp. The illustrations show how a short plug of a substance is dispersed in different transport modes.

Transient flow

But how will a fluid stream with unsteady composition be affected when it is transported in microfluidic channels? Or if we switch between different solutions? These questions can be answered by analyzing the transient propagation of concentration pulses. The convection-diffusion equation (Eq. 2.28) shows that in this case all three terms contribute to the equation, and an exact solution would depend on two dimensionless parameters, St and Pe . This makes it more complicated to formulate a universal description. However, depending on which phenomena are

dominating it is possible to separate different transport modes, and provide simpler models to describe each of them [15]. This depends on two aspects, the Peclet number and the ratio of channel length and radius L/r (Figure 2.5). Here the Peclet number represents the ratio of convection along the channel axis (axial) and diffusion across its cross section (radial). But since the convection ($\propto t$) and diffusion ($\propto \sqrt{t}$) are scaling differently, the channel length has to be also considered in order to determine the right transport model.

Let's look first at the case of a low Pe number, where the flow is slow and the diffusion is fast. If the channels are relatively short, the output is primarily dominated by diffusion (**Pure axial diffusion**). However, when the channel length is increased, the convection will eventually catch-up with diffusion, due to their different scaling. In this case, the convection dominates the axial transport, but the radial transport is still ruled by the diffusion, which means that the concentration over the cross-section of the channel is constant. (**Axial convection, radial diffusion**). the border between these modes is approximately at $Pe \approx 0.4r/L$.

If we increase the flow and Peclet number, the radial diffusion cannot keep up with convection. In case of very fast flow and short channels, the pressure driven fluid stream is stretching the substance pulse into a parabolic shape, while diffusion does not have time for any significant action. Then the dispersion is only due to **Pure convection**. When the channels are made sufficiently long, both diffusion and convection are entering the process. Convection is stretching the concentration pulse and diffusion is mixing it in radial direction. This was studied by the British physicist Sir G. I. Taylor in the 1950's [16], who found that the interplay between axial stretching and radial diffusion causes the injected fluid plug to be smeared in the same way as diffusion does, but with a very much higher diffusion coefficient. This dispersion mode has been coined after him as **Taylor dispersion**. The effectively increased axial diffusion coefficient D_{eff} is called a Taylor dispersion coefficient

$$D_{eff} = \frac{r^2 v_{aver}^2}{48D} \quad (2.31)$$

In contrast to the molecular diffusion coefficient D , the Taylor dispersion coefficient is not a materials property, but depends on the geometries and flow rates in the tube. It is interesting to note that molecular diffusion has an inverse effect on the Taylor dispersion (Eq. 2.31). A higher D corresponds to lower dispersion. Pure Taylor dispersion neglects the axial diffusion, but when the Pe numbers are lower, both the contribution of Taylor dispersion and of molecular diffusion should be considered (**Taylor-Aris dispersion**), with the dispersion coefficient given by eq. 2.32.

$$D_{eff} = D + \frac{r^2 v_{aver}^2}{48D} \quad (2.32)$$

When it comes to practical calculations, it is important to notices that the above given coefficients (Eq. 2.31, 2.32) and boundaries between the dispersion modes are for

circular capillaries. In case of other channel shapes, geometry specific correction coefficients have to be used, while the scaling laws still hold universally. For example, for high aspect ratio channels with width w , the Taylor-Aris dispersion becomes [17].

$$D_{eff} = D + \frac{w^2 v_{aver}^2}{210D} \quad (2.33)$$

In case of more complex geometries and transition region between the dispersion modes, it is often most efficient to use numerical computer simulations (discussed in a later chapter).

In all transport models (Figure 2.5) other than pure convection and the transition region neighboring it, the concentration can be considered constant across the channel cross-section (radially), and it varies only along the channel axis, i.e., dispersion and transport can be described as a one dimensional system.

This simplifies the mathematical representation. In all these cases, dispersion is described as diffusion, whether molecular or Taylor's.

If we want to calculate how a solution of variable composition is affected by the transport through a channel, the notion of signals and system, where time dependent concentration takes the role of a signal, and diffusion in the channel takes the role of a system, can become useful. In this notion a system acts on the input signal, turning it into an output signal. The diffusion process is a linear-time invariant (LTI) system, meaning that i) changing concentration at the input would change the concentration at the output proportionally, and ii) the channel behaves exactly the same at different times. LTI systems have several useful properties. They can be described entirely by their impulse response function, which reflects how the system transforms an infinitely narrow input pulse (delta impulse). In case of diffusion, or Taylor dispersion, such a pulse would spread and evolve into a Gaussian.

$$C_{sys}(x, t) = \frac{1}{\sqrt{4\pi Dt}} \exp\left(-\frac{x^2}{4Dt}\right) \quad (2.34)$$

where D is the dispersion coefficient and t is time. If we consider a channel with length L and average velocity v_{aver} , the spatial coordinate can be turned into a time delay. $t = (L - x)/v_{aver}$, giving eq. 2.35.

$$C_{sys}(t) = \frac{1}{\sqrt{4\pi Dt}} \exp\left(-\frac{(L - tv_{aver})^2}{4Dt}\right) \quad (2.35)$$

LTI implies that in this case the output signal of the system is a convolution of input signal and impulse response of the system.

$$c_{out}(t) = c_{inp}(t) \otimes \mathcal{C}_{sys}(t) = \int_{-\infty}^{\infty} c_{inp}(\tau) \mathcal{C}_{sys}(t - \tau) d\tau \quad (2.36)$$

LTI systems can be represented also in a frequency (Fourier) domain, where the convolution integral turns into a simple multiplication of the two spectra of the input signal and the impulse response.

$$c_{out}(\omega) = c_{inp}(\omega) \cdot \mathcal{C}_{sys}(\omega) \quad (2.37)$$

Each spectrum can be found using the Fourier transform.

$$c(\omega) = \int_{-\infty}^{\infty} c(\tau) e^{-i\omega\tau} d\tau \quad (2.38)$$

If we assume that axial convection is larger than dispersion, as it usually is, the impulse response of the channel would become

$$\mathcal{C}_{sys}(t) \approx \frac{1}{\sqrt{4\pi DL/v_{aver}}} \exp\left(-\frac{(L - tv_{aver})^2}{4DL/v_{aver}}\right) \quad (2.39)$$

which has Fourier transform

$$\mathcal{C}_{sys}(\omega) \approx \frac{1}{v_{aver}\sqrt{2\pi}} \exp\left(-\frac{DL}{v_{aver}^3}\omega^2\right) \exp\left(-i\frac{L}{v_{aver}}\omega\right) \quad (2.40)$$

The magnitude of this spectrum is

$$|\mathcal{C}_{sys}(\omega)| \propto \exp\left(-\frac{DL}{v_{aver}^3}\omega^2\right) = \exp\left(-\frac{\omega^2}{\omega_p^2}\right) \quad (2.41)$$

This function has larger values in case of low frequencies (ω) and low values in case of higher, which means also that the channel acts as a **chemical low-pass filter** for concentration signals, letting to pass slow concentration waves, while damping sharp changes. Parameter ω_p can be referred as a **cut-off frequency** of the filter [18].

$$\omega_p = \sqrt{\frac{v_{aver}^3}{DL}} \quad (2.42)$$

The cut-off frequency is higher with fast flow (no time for dispersion) and is lower with a higher dispersion coefficient and longer channels.

In the context of the research of this thesis, the chemical low-pass filter has been used in a microfluidic diluter (Paper I & II), where it smoothens fast pulses to a constant

concentration level. Note that if fast solution exchange is desirable (Multifunctional pipette (Paper III)), the dispersion effects are a limiting factor.

2.1.3 TEMPERATURE

Temperature is also affecting chemical and physical processes. It describes the motional energy of molecules, which affects their diffusion and reaction rate (Arrhenius law), as well as the chemical equilibria. Thermal transport is very similar to the convection-diffusion equation (Eq. 2.27)

$$c_p \frac{\partial T}{\partial t} = -c_p \vec{v} \cdot \nabla T + \frac{k}{\rho} \nabla^2 T + P \quad (2.43)$$

where c_p is the specific heat capacity, k is the thermal conductivity, ρ is the density and P is the spatial heating power. Re-arranging the equation gives

$$\frac{\partial T}{\partial t} = -\vec{v} \cdot \nabla T + \frac{k}{\rho c_p} \nabla^2 T + \frac{P}{c_p} \quad (2.44)$$

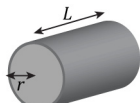
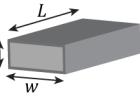
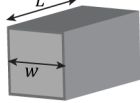
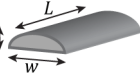
where $D_T = k/\rho c_p$ is the thermal diffusivity. Even though the thermal convection-diffusion equation is exactly the same as for the concentration case, there is one significant dissimilarity, which is especially important in the microfluidics realm: the difference of the diffusion constants between different materials. Molecules diffuse readily in liquids, but they do not enter into most solids (their diffusion constant is close to zero). Therefore we can consider that molecular diffusion occurs only inside channels, while, on the other hand, temperature is very similarly conducted by solids and liquids. For example, the thermal diffusivities in water and glass are $1.4 \cdot 10^{-7} \text{ m}^2/\text{s}$ and $3.4 \cdot 10^{-7} \text{ m}^2/\text{s}$, respectively. This means that both the liquid and the device have to be considered when calculating heat transport in microfluidics. For practical purposes this is mostly done by using finite-element modeling (FEM). In comparison to molecular diffusion, thermal diffusion is much faster. This is favorable in case precise temperature control is needed, due to the fast thermal equilibration of the liquid to the device temperature. Fast diffusion makes it, on the other hand, harder to generate thermal gradients (Figure 2.4). In order to achieve a sufficiently high Pe number, the channels have to be larger and flow faster. Nevertheless, thermal gradients established in microfluidic devices have been exploited to study, for example, developmental control mechanisms in fly embryos [19]. Thermal diffusion has been considered in the design of the optofluidic thermometer (Paper VI), where the flowrates had to be chosen to ensure confinement of fluorescent dyes, but would at the same time allow thermal equilibration.

2.2 MICROFLUIDICS *VERSUS* MICROELECTRONICS

2.2.1 ANALOGIES

Microfluidic and microelectronic device are not only fabricated in a similar way, they also hold similarities in the circuit theories used to describe them. With slight modifications, this analogy provides a variety of useful tools for designing and analyzing microfluidic circuits. Equation 2.26 describes the flow rate dependence in a microfluidic channel, where the flow rate is proportional to the pressure difference at the channel ends and to a parameter depending on channel geometry and viscosity. This is corresponding to Ohm's law in electronics, which describes the proportionality between current and a voltage difference. Fluidic analogies for voltage, current, current density and charge would be pressure, flow rate, flow velocity and fluid volume, respectively. The channel geometry and viscosity dependent proportionality parameter is called "hydrodynamic resistance". Similar analogies exist also for other passive circuit elements capacitor and inductor (Figure 2.6). Hydrodynamic capacitance describes which volume of a liquid can be placed into a "liquid capacitor" per unit of pressure increase. In physical terms, the "liquid capacitor" can correspond to an elastic tube, which is enlarged in volume when pressurized, or to air-bubbles in a channel, which can be compressed. Inductance corresponds to mechanical inertia of the flow.

Table 2.1. Most common channel and tube geometries for microfluidics and their respective hydrodynamic resistances [10].

Geometry	Channel resistance	Figure
Circular	$R = \frac{8}{\pi} \eta L \frac{1}{r^4}$	
Rectangular	$R \approx \frac{12}{1 - 0.63(h/w)} \eta L \frac{1}{h^3 w}$	
Square	$R = 28.4 \eta L \frac{1}{w^4}$	
Parabolic	$R = \frac{105}{4} \eta L \frac{1}{h^3 w}$	

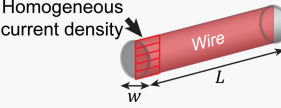
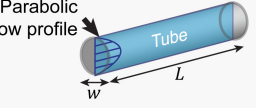
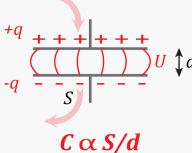
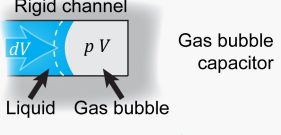
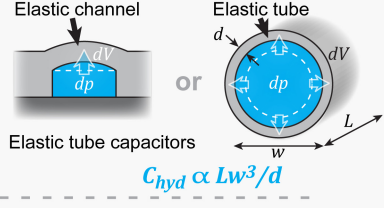
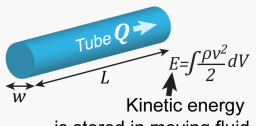
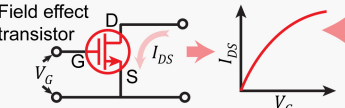
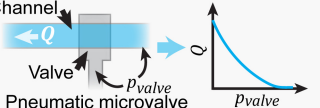
	Electronics	Fluidics
Flow properties	Voltage / U (Unit: V) Charge / q (Unit: C) Current / I (Unit: A) Current density / σ (Unit: A/m^2)	Driving potential Transported substance Transport rate Transport intensity
Circuit properties	Resistance / R (Unit: Ω) <i>Ohm's law</i> $I=\frac{U}{R}$	Pressure / p (Unit: Pa) Fluid volume / V (Unit: m^3) Flow rate / Q (Unit: m^3/s) Flow velocity / v (Unit: m/s)
Circuit elements	Capacitance / C (Unit: F) $dq=CdU$	Compliance / C_{hyd} (Unit: m^3/Pa) $dV=C_{hyd}dp$
	Inductance / L (Unit: H) $dU=Ldi/dt$	Inertia / L_{hyd} (Unit: $Pa s^2/m^3$) $dp=-L_{hyd} dQ/dt$
	 $R \propto L/w^2$	 $R_{hyd} \propto L/w^4$
	 $C \propto S/d$	 $C_{hyd} = p_0 V_0 / p^2$
		 $C_{hyd} \propto Lw^3/d$
	Current generates magnetic field $B \propto I$ $E = \int \frac{B^2}{2\mu_0} dV$ Magnetic field contains energy	 $L_{hyd} \propto L/w^2$
		

Figure 2.6. (On previous page) Analogies between electronics and fluidics.

Besides passive components, active components, like valves, are also commonly found in microfluidic systems, allowing modulation of the fluid flow. Pneumatic analogs for digital logics, latches and even fluidic processors have been reported [20-22].

2.2.2 CIRCUITS

Similarly to electronics, these microfluidic elements can be combined to circuits with different properties. The most common of such circuits is a simple network of channels, which corresponds to a network of flow resistors, where pressures are applied to the inlets. In order to find the flow rates in such a system, Kirchoff's rule, stating that the sum of flows to every circuit node has to be zero (incompressible fluid and channel), can be applied. For practical calculations we can first redraw the system in the way shown in figure 2.7, by grouping inlets/outlets and internal nodes of the circuits. The resistances of each flow resistor, and the pressures at the inlets, are known, thus the complete flow pattern can be calculated after the pressures at the internal nodes have also been found. This requires solving a linear equation system. To compose such an equation we consider linearity, which means that the flow in every resistor can be expressed as a superposition of two flows, each starting from a different end of the resistor. For mathematical simplicity we can replace the resistances by conductivities $G = 1/R$, then $Q = G \cdot p$. Now we can write the equation for an internal node i , using Kirchoff's current rule: the sum of the outflows from the node to every other node, and the inflows from every other node to the node has to be zero. For the node i this can be written as eq. 2.45.

$$\underbrace{-\left(\sum_{j=1}^m g_{ji} + \sum_{j=1}^n G_{ji}\right)}_{\text{outflow from the node } i} p_i + \underbrace{\sum_{j=1}^m g_{ji} p_j}_{\substack{\text{inflow from} \\ \text{other internal} \\ \text{nodes to node } i}} + \underbrace{\sum_{j=1}^n G_{ji} P_j}_{\substack{\text{inflow from} \\ \text{input nodes to} \\ \text{node } i}} = 0 \quad (2.45)$$

This system of m linear equations can be re-arranged into a matrix form,

$$\underbrace{\begin{pmatrix} -\sum_{i=1}^m g_{i1} - \sum_{j=1}^n G_{j1} & \dots & g_{1m} \\ \vdots & \ddots & \vdots \\ g_{m1} & \dots & -\sum_{i=1}^m g_{im} - \sum_{j=1}^n G_{jm} \end{pmatrix}}_g \begin{pmatrix} p_1 \\ \vdots \\ p_m \\ \vec{p} \end{pmatrix} = -\underbrace{\begin{pmatrix} G_{11} & \dots & G_{n1} \\ \vdots & \ddots & \vdots \\ G_{1m} & \dots & G_{nm} \end{pmatrix}}_G \underbrace{\begin{pmatrix} P_1 \\ \vdots \\ P_n \\ \vec{P} \end{pmatrix}}_{\vec{P}} \quad (2.46)$$

which makes it convenient to solve

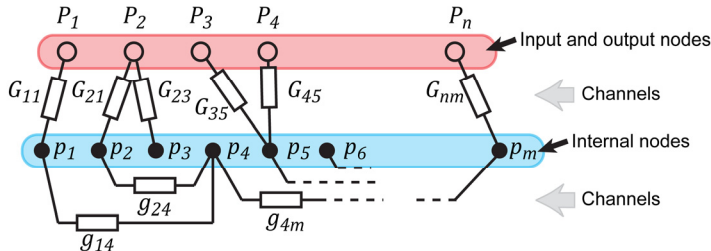


Figure 2.7. Calculating flows in arbitrary channel networks. The network has n inlets and outlets, with defined pressures P_i , and m internal nodes with pressures p_j which shall be found. Each internal node i can be connected with another internal node j through a resistor with conductance g_{ij} , or with inlet k through a resistor with conductance G_{ik} . Nodes that are not connected have zero conductances between them. Also $g_{ii} = 0$.

$$\vec{p} = -\mathbf{g}^{-1} \mathbf{G} \vec{P} \quad (2.47)$$

Other circuit elements, such as fluidic capacitors and inductors can be also incorporated in the calculation by replacing resistances by impedances with complex values.

In the following we consider a few important circuits for microfluidics design, where multiple different types of elements have been combined (Figure 2.8). Since these are not just resistor networks, their response has also a temporal component, which shall be considered while designing the fluidic switching systems. The first example is a tube or a channel, with elastic walls, or with a compressible fluid in it. Such a tube acts as a series of resistors and capacitors (Figure 2.8A), known also as a RC-line, which slows and delays any pressure signal applied through it. Pressure propagation in such a tube is described by the differential equation (Eq. 2.48)

$$\frac{L^2}{RC} \frac{d^2 p}{dx^2} = \frac{dp}{dt} \quad (2.48)$$

If we turn it into a dimensionless form, we can see that the equation depends only on one dimensionless parameter $\tau = RC$. The higher the RC constant the longer and slower is the response. This is an important consideration in fluidic switching systems, such as the multifunctional pipette presented in paper III . Similar RC circuits are involved in pneumatic valves (Figure 2.8B), since deflecting the valve will require a certain volume of fluid (capacitance), which is transported through the channel (resistance).

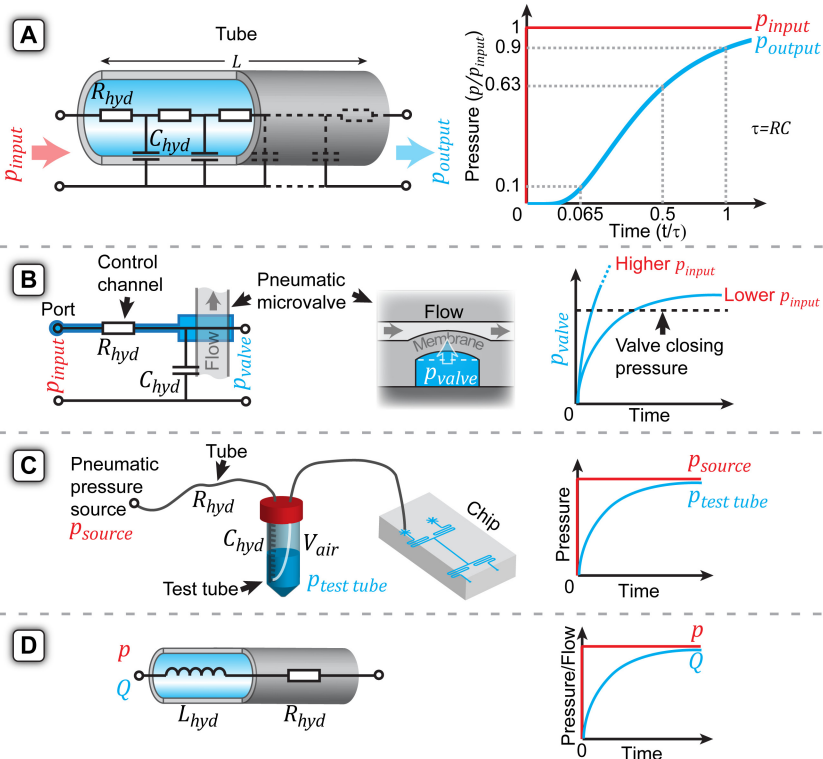


Figure 2.8. Circuit elements in a microfluidic design. **(A)** Pressure propagation in an elastic tube. **(B)** Control of microvalves. **(C)** Controlling pressures in a supply tube. **(D)** Hydrodynamic inductance.

$$p_{out} = p_{in} \left(1 - e^{-\frac{t}{\tau}} \right) \quad (2.49)$$

RC constant ($\tau = RC$) determines how fast these valves can be actuated.

Here, faster valve closure can be achieved by using higher control pressure, since the necessary pressure level would be reached sooner. The RC constant itself, however, is independent of pressure. This has been a consideration in the design of the microfluidic diluter (Paper I). The third example involves pressure driven flow from a test tube (Figure 2.8C). In order to establish a flow, the test tube has to be pressurized, which involves a gas flow from the supply. In case of small pressures, $C \approx V_0/p_0$. The last example shows a microfluidic analogue to an RL circuit, which is describing the inertia of the flow (Figure 2.8D). The hydraulic inductance can be expressed as $L = 2E_{kin}/Q^2$, which in case of a circular tube would be $L = 4\rho l / 3\pi r^2$. The time

constant of such a circuit is $\tau = L/R$, and it scales with the channel size as $\propto r^2$, meaning that the significance of inertia is dropping rapidly with shrinking dimensions.

2.2.3 DIFFERENCES

Even though there are many analogies, fluidics is so far having difficulties to fully mimic highly integrated electronic circuits. This is due to a few, essential differences between these two domains of technology (Figure 2.9). The most important one is the way how information is carried and processed. In electronics, it is electric potential and current, carried by a single particle: the electron. In fluidics it is the pressure and the fluid flow, but with the exception of some micropneumatic control systems [22], interesting information is usually carried neither by the flow nor by the pressure, but by the chemical composition. In contrast to the electron, there are nearly infinite numbers of molecules and mixtures possible. This has an implication: in fluidics it is not enough to convey information by waves of potential, but liquid has to actually travel through the system, which is much more time consuming and makes it hard to efficiently connect different chips with macroscopic tubing. The ease of interconnectivity has been the foundation for applicability of microelectronics. Microchips, which contain many microscopic transistors and require complex and expensive manufacturing are universal building blocks that are easily connected by macroscopic wires and circuit boards to create a particular functionality. Therefore great applications emerged (literally) from garage projects, for example the personal

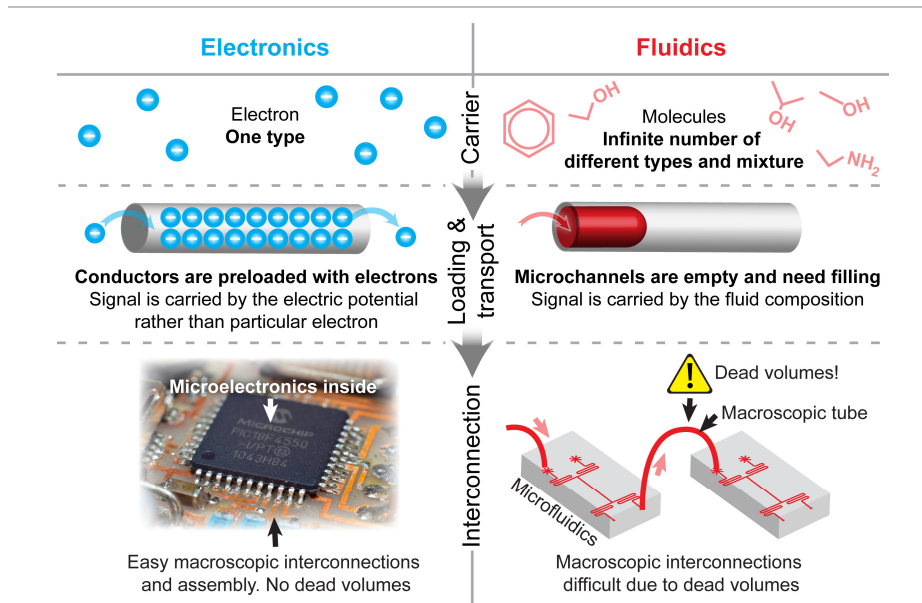
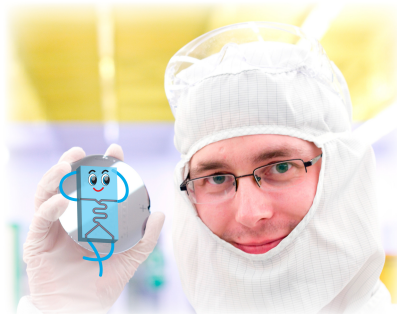


Figure 2.9. Differences between microelectronics and microfluidics

computer. Modular microfluidic constructors have been also developed, but comprised circuits with significantly larger channels (several 100s of μm) [23-24].

Another important difference is that the function of electronic circuits usually does not depend on the length of the interconnections (except very high frequency electronics), while in fluidics, the interconnections are also entangled with the properties of the circuit - their length, volume and fluidic resistance has to be considered. This restricts the flexibility of the assembly. It is typically needed that all functions of the system are incorporated into one chip, specifically created for a desired purpose. Therefore facile and low-cost methods to prototype and fabricate chips are needed to promote the development of new devices for various applications. Closest to this ideal is PDMS microfluidics, which has gained huge popularity among developers [25]. PDMS microfluidics is more thoroughly described in the third chapter. Hopefully, currently emerging rapid prototyping techniques (e.g. 3D printing) will lead to even simpler methods for designing and creating microfluidic systems.



3. METHODS

Dust particles, common in our ambient atmosphere, can be significantly larger than microstructures, therefore microfabrication has to be performed in a highly clean environment - a cleanroom. Special overalls are required for operators to protect the samples from the biggest source of contamination - us. The photo shows the author in the MC2 cleanroom at Chalmers, holding a silicon master used to manufacture PDMS multifunctional pipettes.

3.1 FABRICATION OF MICROFLUIDIC DEVICES

Most typical microfluidic devices are containing features that vary in size over 3-to-7 orders of magnitude: a cm scale chip, mm scale solution reservoirs and interface ports, and 100-10 μm scale channels. However, microfluidics can also bridge with nanofluidics, bringing the channel size down to the nanometer scale. It is hard to fabricate all of them with a single technique. Therefore, combinations of various tooling technologies are required [26]. For example, the main device in this work, the multifunctional pipette, has been fabricated using a mold which consists of two parts - a microfabricated master to define the microchannels, and a milled cavity to give the device its shape and define the solution reservoirs (Figure 3.1). The following section gives an brief overview of fabrication technologies for microfluidic devices.

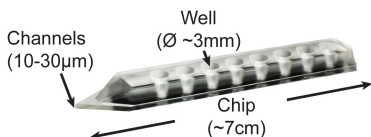


Figure 3.1. Size scales of a microfluidic device, visualized on the example of the Multifunctional Pipette.

Key element of most current microfluidic devices is a network of small channels, where liquid handling occurs. Notable exceptions are droplets on surfaces, paper and thread microfluidics. Apart from rare techniques, which allow for generation of channels directly [27], most approaches to form close channels involve two common

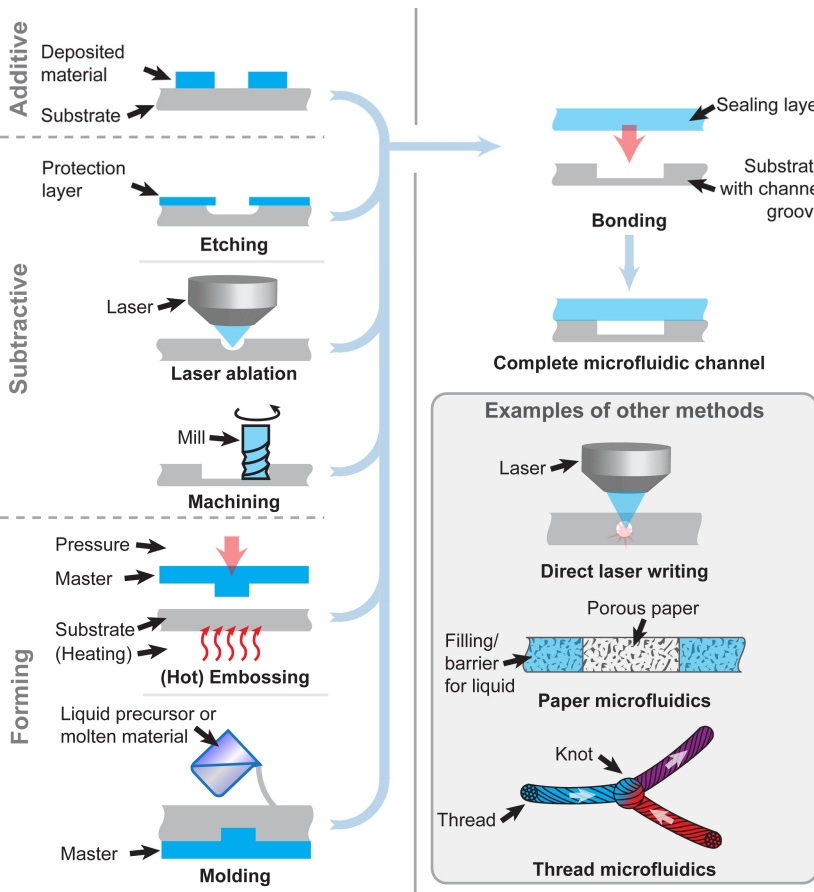


Figure 3.2. Fabrication of microfluidics devices.

steps - fabrication of a channel groove and subsequent sealing of its opened side with another layer of material (Figure 3.2). This procedure can be repeated to build multilayered channel structures. A large variety of techniques has been developed to fabricate channels and seal them in numerous different materials.

In general, fabrication techniques can be divided into three groups: **additive**, where materials are selectively added and gaps between them form channels; **subtractive**, where materials are selectively removed, and **forming**, where materials are shaped with the help of a template ("master").

3.1.1 ADDITIVE TECHNIQUES

The most common and well established way to define microstructures is through a photolithographic process (described in detail later), where a thin film of a light sensitive polymer (photoresist) is applied on a flat surface. A pattern is created by illuminating the photoresist through a photomask, followed by selective removal (development) of either exposed or unexposed parts of the resist. In most photolithographic applications, the forming resist pattern is used as a physical mask for further processing, such as deposition or etching. In microfluidics, the resist layers can be used directly as building material to define the device. Especially popular is the negative epoxy photoresist SU-8. Multiple SU-8 layers can be fabricated on top of each other, and also bonded thermally [28]. This method allows fabrication of high precision, chemically resistant devices. Shortcomings are the expensive materials and instrumentation required. While typical lithography is limited to thin solid coatings of photoresists, stereolithography, a related technique, (patented 1984 by C.W. Hull) [29], works in a liquid bath of photopolymer. This allows the sample to be moved vertically, while the strong optical absorption of the polymer ensures that the photoreaction occurs only in a very thin layer on the surface, which is scanned by a laser. By this layer by layer approach it is possible to build large 3D structures. This technology was expensive, and accessible only for industrial prototyping, until recently, when affordable 3D printers have become available [30]. Stereolithography has been also used to make high precision (about $\sim 40\mu\text{m}$) objects composed of multiple materials [31]. Similarly, multiphoton lithography is a technique to build 3D structures optically, but with significantly smaller feature size ($< 1 \mu\text{m}$) [32]. This very sharp point is achieved by non-linear absorption of a focused femtosecond laser. Other, inkjet-like 3D printing techniques, have found applications to build hydrogels for tissue scaffolds [33] and even assemble multiple cell types, which can be used in the future for regeneration of tissue [34]. Lately, customized low-cost 3D printed reactionware has been used for chemical synthesis [35]. It is a visionary example, showing the transition of 3D printing technology from model making to low-cost prototyping and manufacturing of functional scientific instrumentation. Similar developments would be highly desirable also for microfluidics. So far, low-cost methods lack the resolution, while high resolution multiphoton lithography is expensive, slow and restricted to small structures. However, affordable 3D printing is already available to make somewhat larger 'millifluidics', which can be applied to create interfaces to microfluidic devices [36]. It can be expected that 3D printing and related techniques will also revolutionize the fabrication of microfluidic devices, as it anticipated in other areas of manufacturing. In some people's opinion, the third industrial revolution will be based on 3D printing and mass customization [37].

3.1.2 SUBTRACTIVE TECHNIQUES

The most commonly used subtractive technique in microfabrication is **etching** - a chemical removal of material. In order to define features, the substrate is typically patterned, using a photoresist. Development creates openings in the resist layer, which

define where the etching takes place. Depending on the chemical environment, etching procedures are divided into **wet etching** in solutions and **dry etching** using gases and plasmas [38]. The materials most commonly etched are inorganic, such as oxides, silicon and glass, the latter two being the most significant for practical microfluidic applications [39].

Glass is usually wet etched, using concentrated hydrofluoric acid (HF). With 48% HF, the isotropic etch rate at room temperature is about 8 $\mu\text{m}/\text{min}$ [40]. Since glass is an attractive material for microfluidics, and there is a lack of alternative fabrication processes, HF etching is used widely. It has serious disadvantages, though, such as health risks, but also the isotropic etching profile, which can only produce shallow, wide channels with round edges. Since photoresists do not withstand HF, an evaporated sacrificial metal layer (e.g. Cr/Au) must be used as etching masks. This is an additional expensive process step.

Silicon has long been a standard material for the electronics industry. Its numerous processing techniques are well established for microelectronics fabrication. From the microfluidics and MEMS prospective, the most interesting technique is **deep reactive-ion etching (DRIE)**. This process was patented by Robert Bosch GmbH 1992 [41]. It allows etching of very high aspect ratio structures with nearly vertical side walls. This dry plasma etching process uses two steps, nearly isotropic chemical etching with SF₆, followed by surface passivation with an inert plasma deposited fluoropolymer. This cycle is repeated, until the desired depth is reached [42]. In order to introduce directionality, the substrate is biased, which causes vertical bombardment of the passivation layer by ions. This removes the polymer layer selectively from the bottom of the structure, while having less effect on the side walls. In this way etching proceeds only from the bottom. Number and length of cycles are determining overall etch speed and smoothness of the side walls. DRIE can produce deep (100s of μm), high aspect ratio (>25), uniform (~5%) structures at moderate speed (~6 $\mu\text{m}/\text{min}$) and with good selectivity on silicon over the photoresist etch mask (>50:1) [42]. If higher uniformity is needed, DRIE can be performed on silicon on insulator (SOI) wafers (<1%). In this case the etching proceeds until it reaches a buried oxide layer, which defines the final etch depth. Disadvantage of SOI wafers is their very high cost (almost 10x as high as regular Si wafers [43]), but it can be an option to fabricate precision masters used for replica molding [44]. The DRIE process has been adopted also for glass, using CHF₃ as etching gas, but it suffers from poor selectivity, and requires an anodically bonded silicon wafer as an etching mask [45]. The aspect ratio is also much lower compared to silicon (wall angle of about 85°). Therefore, efforts to perform DRIE on glass are only justified in specific cases.

Laser ablation is a technique, where high power laser radiation is used to remove material [46-47]. The exact ablation mechanism depends on the laser and the substrate material, but in general it can be photochemical (UV lasers) or thermal (IR laser). Depending on the instrument, ablation can occur as a parallel process, where the entire structure is illuminated through a mask, or as a serial process, where the beam is scanned over the pattern to be written. Typical substrates are polymers, but

also glass has been laser ablated, even though it requires more care, to avoid thermal stress and cracking [48]. Laser processing can be combined with post processing, such as wet etching. Laser ablation has been used for both fabrication of channel networks as well as for additional process steps, such as creation of interconnects in multilayered PDMS devices [49]. Low-cost commercial cutters are based on CO₂ lasers. They can produce ~100 μm channels with a surface roughness of a few μm in PMMA. Higher resolutions can be obtained with pulsed excimer, Nd:YAG or Ti:sapphire lasers, which can ablate in sub-μm steps [50]. Disadvantages of laser processing are channel roughness, and uncontrollable surface properties due to radiation damage and debris, which is deposited around the ablation site. Main advantage is the single-step fabrication of channel structures from design to finished chip, without the need for photolithography. This makes laser ablation a good candidate for rapid prototyping of microfluidic devices.

Mechanical machining is mostly associated with manufacturing of macroscopic goods, but micromilling can be equally competitive for microfluidic purposes [51-52]. For example, a high performance milling machine with 1 μm movement precision and 50-400 μm diameter carbide milling bits has been used to machine a brass molding master, featuring 20 μm wide and 400 μm high channel structures (aspect ratio 20), with vertical side walls having an average roughness of <100 nm. PMMA CE chips produced from this master had a similar separation performance compare to the ones fabricated with a LIGA-made master. If needed, the machined metal structures can be further smoothed, for example, by electrochemical polishing [53]. For engraving of channels, milling bits with a diameter down to 5 μm exists, even though for economical reasons their high price (>1'000kr/pcs) and wear rate should be considered [54]. Examples of milled microfluidic devices in aluminum with channel sizes ranging from 100 to 700 μm, have found use in, for example, chemical synthesis of polymers [55] and fluorescent microparticles [56]. Like with laser ablation, the advantage of milling is that the structures can be created from the design in a single process. Furthermore, one machine can produce features with greatly different heights, which is rarely possible with other techniques. Disadvantages are the low throughput, high cost of machinery, and rapid wear of tools.

3.1.3 FORMING TECHNIQUES

The world of low cost disposable microfluidic devices is ruled by the different forming techniques for polymers. All of them share a common feature: a template, also called master or mold, is used to define the shape of a soft, or softened polymeric material, which is thereafter hardened, and released from the template. The molds themselves have to be manufactured using other techniques.

Casting (also reactive injection molding, or replica molding) is the simplest method, with minimal capital investment required to start. This is the reason why it has become popular for microfluidic chip fabrication in academic laboratories. Casting is used to create devices in thermosetting and elastomeric materials, starting with a liquid pre-polymer, which is poured onto the master or injected into the mould cavity,

followed by curing. Heat or UV-light cross-links the pre-polymer, turning it into hard plastics or rubber, which is then removed from the mold. A great advantage of casting is that it requires no special equipment other than the mold, which can be easily fabricated with high precision using lithographic patterning of photoresists (e.g. SU-8). Since the pre-polymer mixture is of low viscosity, it usually fills the mold without problems. The relatively long setting time makes the process robust and easy to reproduce manually. However, this last aspect turns into a major disadvantage when trying to use the technique for high throughput production, since the curing time can be on the order of hours, compared to injection molding, which can complete a cycle in seconds. All devices in the present work have been made using casting or reactive injection molding of PDMS.

Injection molding is a well established industrial method to manufacture macroscopic parts in thermoplastic materials. Similar to casting, a soft polymer mass is injected into a mold where it solidifies, adopting the shape of the mold. Instead of chemical reaction, the liquid/solid state of a thermoplastic is controlled by heating and cooling it around its glass transition temperature (T_g). Since the required temperature change is relatively small, injection molding can have very short production cycles, limited only by thermal diffusion. Due to the viscosity of molten polymers, high injection pressures (~1000 bars) are required [57]. Many other aspects have to be considered when adopting injection molding for a new design, such as the temperatures of plastic and mold, injection rate and pressure, cooling times and holding pressures [58-59]. The design has to also consider the release of the final solid part. Thermal and flow "memory" of high molecular weight polymers can cause uneven shrinkage, stress and bending. In order to cope with this multi-dimensional optimization problem, specific softwares exist to model the injection molding process. Compared to "classical" injection molding on the macro scale, microinjection molding has its own additional requirements, like the use of an evacuated mold, cycling of the mold temperature (the VarioTherm process), used to avoid cooling of the polymer before it has managed to fill the small features. On one hand, very high costs for capital equipment, the fabrication of the mold cavity, and the required process optimization have rendered injection molding essentially inaccessible to academic researchers. On the other hand, low maintenance and material costs, high throughput and automated manufacturing, as well as a wide variety of different material, has made injection molding the method of choice for larger-scale industrial production of microfluidic devices.

Embossing (also nanoimprint) is, like injection molding, used to shape thermoplastic materials, but the extent of geometrical transformation of the material is less [60]. The process starts with the insertion of a plastics piece between two mold plates, where it is heated until softening (around T_g). Thereafter the plates are pressed together, shaping the softened material, which is then cooled to solidify. Microstructure imprinting can be performed in vacuum to avoid defects by trapped air. The material flow is in this case much smaller compared to injection molding, therefore it causes less stress. In general, hot embossing is significantly simpler than injection molding, but also with lower throughput and a more restricted range of usable geometries. Since high stress

is involved due to pressing, the masters have to be stronger (typically DRIE etched silicon or electroplated metal), than the photoresist patterns used for PDMS casting. This additional difficulty makes embossing less common for prototyping. Nevertheless, hot-embossing is an excellent choice for relatively easy reproduction of fine (sub μm) and high aspect ratio structures in thermoplastics.

In conclusion, which choice to make from the above mentioned techniques, depends on geometrical and material requirements. It is also an economic decision determined by the scale of production. Casting is suited for small series (up to 100s of pieces), followed by embossing and injection molding for large scale (in the >10'000 pcs range) [50]. From the materials perspective, casting is limited to curable polymers, while embossing and injection molding can be used with a wider variety of thermoplastics. From the aspect of geometry, casting and injection molding have high flexibility to replicate 3D structures at different size scales in a single process step, being only limited by release-related restrictions. Embossing is suited only for 2D layouts.

3.1.4 CHANNEL SEALING

All of above-mentioned methods can only produce channel grooves. In order to form closed channels, they have to be sealed. Some techniques are reviewed below.

A **Conformal** seal is formed when two flat and smooth surfaces are pressed against each other [61]. This method is very simple, but the resulting devices have generally lower pressure resistance and mechanical integrity. Advantages are the reversibility, which allows the device to be reused, or the ability to chemically or biologically pattern a surface with material from the channels [62-63]. Also, since no pre-bonding treatment is needed, it is easier to integrate microfluidics with a surface which is already covered with a (potentially sensitive) pattern.

Gluing is another well known way to bind surfaces together. In microfluidics, gluing requires precautions to avoid that the channels are contaminated, or even filled, by the glue. An efficient way to transfer liquid glue is stamping from a thin spin-coated layer. For example, UV-curable adhesive and PDMS has been used for sealing [64].

Plasma bonding is a technique to achieve chemical bonding between surfaces after activation with plasma, an ionized gas, which due to its high energy state is extremely reactive. Plasma bonding is a "clean" technique, without the risk of clogging. However, for bond formation to occur between two solid surfaces, smoothness is required to allow molecular level contact. Typically, plasma bonding is used with soft materials. The most widely applied example is oxygen plasma bonding of PDMS to PDMS and PDMS to glass [25], which has also been used to fabricate all devices in the current work. However, plasma treatment is sometimes not sufficient, and the activated surfaces have to be treated further to form a molecular monolayer with suitable bonding chemistry. For example, 3-aminopropyl triethoxy silane (APTES) can be used to assist the bonding of PDMS and PMMA [65] or PDMS and various metals, PP, PE and even Teflon [66]. Tetraethyl orthosilicate (TEOS) has been used for plasma bonding of PMMA-PMMA at low-temperatures [67].

Thermal bonding is used to bond thermoplastic polymers, which are heated slightly above T_g , and pressed together [50, 68]. Care must be taken to avoid deformation of the channel structures. The relatively narrow process window (combination of temperature, pressure, time) is the main disadvantage of this bonding technique, which is otherwise clean, i.e., it neither introduces additional material, such as glue, nor causes surface damage like the plasma bonding technique.

Solvent bonding is similar to thermal bonding, but instead of high temperature, a small amount of a suitable solvent is used to soften polymer surfaces, which are then pressed together. The solvent then diffuses into the bulk material and the bonded polymer hardens again [69-70]. One of the most common examples is ethanol or DMSO/water bonding of PMMA. As with thermal bonding, attention must be paid to avoid excessive softening of the surface, which would deform the channels.

Anodic bonding is used to bond silicon and glass surfaces, which are pressed together under vacuum at elevated temperature (200-450 °C). High voltages (200-1200 V) are applied over the assembly [71], and bonding takes place in about 10-30 min. An alternative way to bond glass without adhesive involves the use of Ca^{2+} ions [72].

3.1.5 OTHER METHODS

In addition to previously described common routes to make microfluidic chips, other method exists, mostly developed for particular purposes. A few examples are mentioned here.

Exciting for rapid prototyping is the direct laser writing into mesoporous glass, using focused pulses of a femtosecond laser [27]. ~40% of the volume of this material consists of pores. Since the method is based on non-linear absorption of light, which locally destroys the material structure, changing the focus height allows to create truly three-dimensional channel networks inside the substrate. The diameter of the circular channels, which is in the range between 10-50 μm , can be controlled by the NA of the objective and the laser power. After writing, the channels are consolidated by high temperature annealing (>1000 °C). This is a rare method by which closed channels are created in a single process step, without need for sealing.

In contrast to all those methods requiring complex machines and materials, some microfluidic devices can be fabricated even at home, using materials as common as paper [73] and yarn [74-75]. Both are functioning based on capillary driven transport in a porous hydrophilic matrix, where circuits can be defined by introducing (printing) hydrophobic wax barriers, or by making knots. These devices do not have high enough precision for most modern laboratory uses, but their almost negligible cost makes them attractive for disposable diagnostics, especially for those whose resources are limited.

3.1.6 MATERIALS

Silicon has well established, but expensive, manufacturing schemes, which involve mainly photolithography and wet and dry etching (DRIE). Since Si is also a substrate

for semiconductor electronics, it is attractive for hybrid electronic-fluidic devices, sensors and MEMS. The advantages of silicon are its high thermal and chemical stability; disadvantages are opaqueness and the planar device geometry, which often requires additional interfacing components.

Glass and quartz are in many ways similar to silicon, but feature optical transparency without auto-fluorescence. Typical fabrication methods are wet etching, which is isotropic compared to the anisotropic DRIE used for silicon. Direct photo-patterning is also possible [76], using pulsed laser treatment, which changes amorphous/crystalline structure of the material and increases the subsequent etch rate. This, in combination with very stable surface chemistry, has made glass prominent for electrically driven (electrokinetic) microfluidics [77-78], in particular for capillary electrophoresis (CE) chips with optical readout.

Thermoplastics are molten by heat and can be then reshaped by injection molding or hot embossing. They are favorable over many other materials, as they are really cheap, optically transparent and easily moldable with minimal geometry restrictions. As biological lab-ware is typically made of thermoplastics, their use and chemical compatibility in biology is well established. All of them are fine in aqueous solutions, but have generally low organic solvent compatibility, different plastics being dissolved by different solvents, especially by hydrocarbons [50]. Most commonly used for microfluidics are PMMA, PC, COP and COC.

Thermoset polymers are solidified by cross-linking, which can be induced by heat or UV-radiation. Once cross-linked these materials will not melt. Therefore channels have to be molded either before curing [79], or by using photo-patterning (e.g. SU-8) or can be etched later using photolithography (e.g. polyimide/Kapton®) [80]. An advantage of thermoset polymers is their high chemical stability (e.g. SU-8, Kapton).

Elastomers, as is evident from the name, are elastic and easily deformable materials. Since elastomers are composed of polymer chains above T_g , they can reflow, but cross-linking limits their overall fluidity. In general, elastomers are favorable, since they are easy to interface, due to their "build in gaskets". They also provide an easy route to fabricate miniature pneumatic valves, invented by Unger & Quake 2001 [81]. The most famous elastomer for microfluidics is PDMS, to which a separate chapter is devoted. Another interesting type of related materials are thermoplastic elastomers (TPEs) [82], which are block-co-polymers (e.g. styrene and butadiene), where one is amorphous and above T_g , and another crystalline acting as a physical cross-linker. Once heated above the melting temperature of crystalline polymer, the entire material melts and acts as thermoplastic, allowing it to be processed as such. After melting, TPEs can have significantly lower viscosity than typical thermoplastics, making their forming easier [82].

Table 3.1. Examples of material costs (Polymer chips are assumed to be 5 mm thick)

Material	Approximate cost	Cost of cm ²
Si	200 sek/4" wafer [83]	2.5 sek
PDMS	500 sek/kg	0.25 sek
Polypropylen	130 sek/kg [36]	0.06 sek
Versaflex TPE	36 sek/kg [82]	0.02 sek

3.1.7 PHOTOLITHOGRAPHY

Photolithography is the main patterning technique in the top-down microelectronics industry. This important application has driven research in optics and photochemicals. Its main results, integrated circuits with more and more transistors (most notably reflected in Moore's law) have been defined by a photolithographic technique. The procedure of photolithography is depicted in figure 3.3. First, a substrate is covered with photoresist. This is typically performed by spin-coating, where photoresist is dispensed onto the substrate, and then thinned by spinning. The final thickness depends on viscosity, spin speed & time, and the rate of evaporation. Alternatives to spin-coating are spray-coating and lamination. After this coating step, the substrate is heated and the solvent evaporated, forming a flat polymer layer, which can be patterned optically, either through a photomask (a parallel process) or by direct writing with a laser scanner [63] (a serial process). Laser scanning is most suitable for rapid prototyping, and masks are superior when multiple substrates need to be processed. For mask-based photolithography there are also several options, depending on quality and feature size required: quartz and deep UV exposure for finest (~ 500 nm feature size), soda lime for intermediate (>1 μm) and polyester films for larger structures (features: >10 μm). The latter is often sufficient for microfluidics, where the channels are several tens of micrometers in size. For comparison, the cost per area of quartz and soda lime masks is about 30, and 20 times higher, respectively, than the polyester film mask [84]. After exposure, the photoresists are developed, meaning that the polymer is selectively removed either from the exposed areas (positive resist) or unexposed areas (negative resist). In the following, the negative SU-8 and positive AZ4562 photoresists, which were used in this work, are more thoroughly discussed.

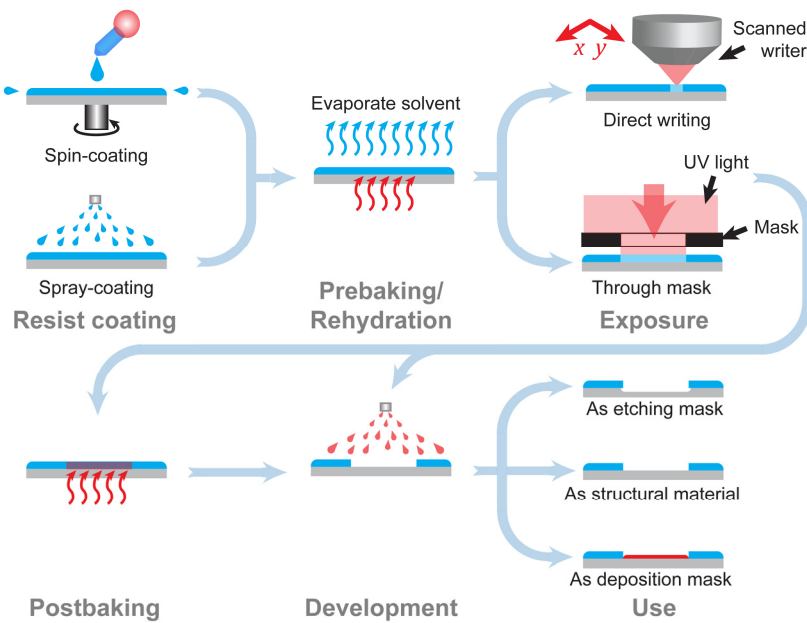


Figure 3.3. Typical photolithographic process

Chemistry of photoresists

SU-8 is a negative, chemically amplified photoresist, originally invented by IBM in the 1980's [85], which is now developed and produced mostly by MicroChem Inc. The key components of the resist are epoxy resin, a photo catalyst and solvent (Figure 3.4). During exposure, the photocatalysts fragments, forming a Lewis acid, which during the post baking step catalyzes epoxy group opening and cross-linking reactions, which eventually renders the exposed part of polymer insoluble in developer (an organic solvent). In fact, hard baked SU-8 becomes completely insoluble in all organic solvents, and can be only slowly removed by oxidation in a plasma or piranha solution. Therefore, SU-8 is primarily a permanent resist, which due to its mechanical strength, optical transparency and excellent adhesion has become widely used as photo-patternable construction material for MEMS and microfluidic devices, as well as for the fabrication of masters for soft-lithography. All microfluidic devices in this work have been made with SU-8 masters. Different resist film thicknesses can be achieved with different formulations of SU-8 in combination with spin speed variations. Film thicknesses in the range of 0.5 to >200 μm are thus obtained in a single-coating cycle [86]. Optimized formulations also exist for improved adhesion (SU-8 3000 series) and highest aspect ratios (SU-8 2000 series).

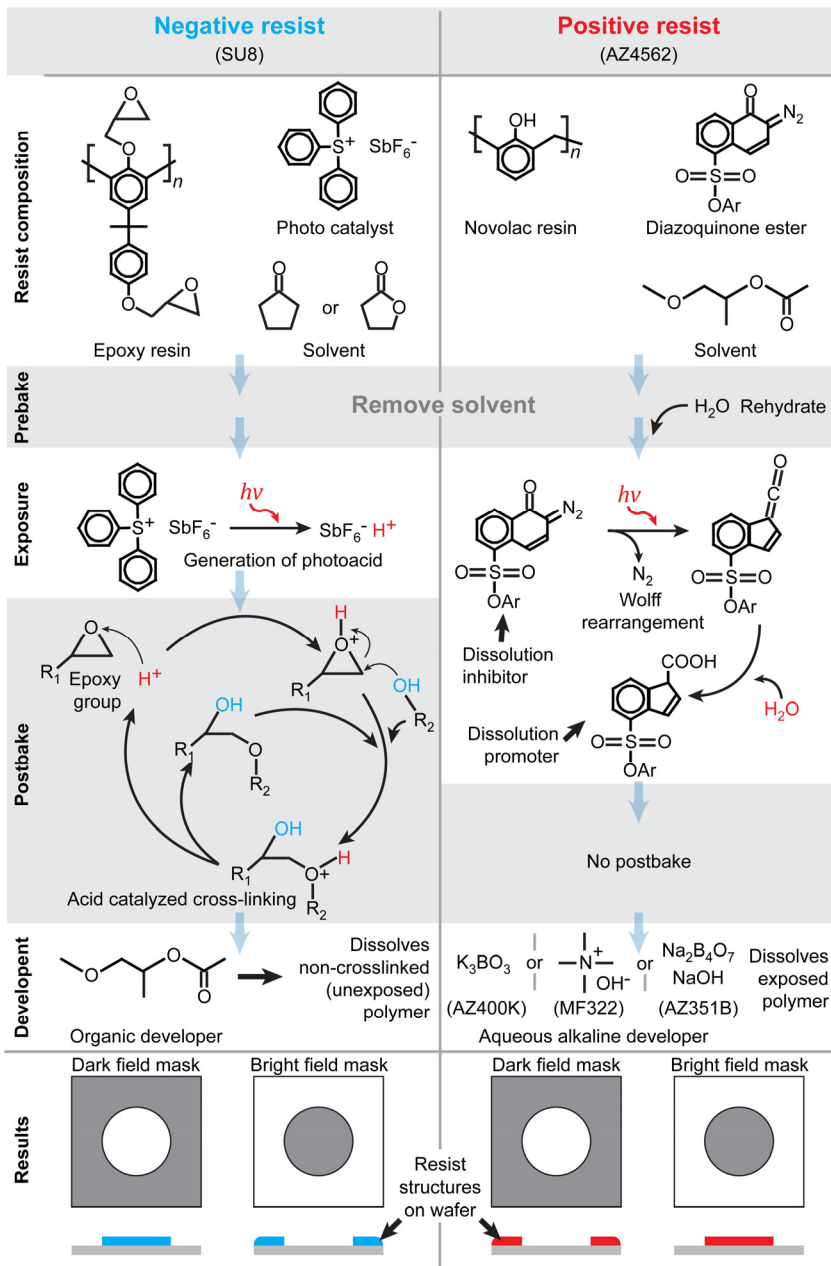


Figure 3.4. Chemistry of photolithography. Examples of negative (SU-8) and positive (AZ4562) photoresists used in the presented research work.

AZ4562 is a positive resist by AZ Electronic Materials GmbH. It is based on a phenolic novolak resin and diazoquinone (DQN resists), where the latter is forming a complex with phenolic OH groups. This hydrophobic complex renders photoresist insoluble in the aqueous developer. Exposure to UV cleaves the diazo group, and in a rearrangement reaction the compound is transformed into a carboxylic acid, which dissociates from the resin and allows it to be removed with alkaline aqueous developer. It must be noted that UV-induced re-arrangement reactions require water to complete. Therefore rehydration, which allows water to diffuse back into the resist after pre-baking is a critical processes step. It happens on negligible time scales in case of thin resists (few μm), but requires up to several hours for thick coatings (tens of μm). DQN resists are suitable for near UV, but not suitable for deep UV exposure, due to strong absorption, which would not allow uniform exposure. This resist is favorable, due to the aqueous development, which pose less health hazards compared to organic solvents (e.g. SU-8 developer). However, it is mechanically much weaker than cross-linked SU-8 and could not be used as constructional material. In microfluidics, positive resists are used for rounded surface elements, since they are not cross-linked. The rectangular structures melt above glass transition temperature, and the liquid resist curves due to surface tension. Rounded channels are the key components in pneumatically actuated microvalves [81], also used in this work (Paper I).

3.1.8 PDMS MICROFLUIDICS

Polydimethylsiloxane (PDMS) is a polymer with a silicon based backbone (-Si-O-) decorated with organic side groups (-CH₃). It has a wide range of uses as a surfactant and anti-foaming agent in food processing, cosmetics and herbicides [87], as structural material for medical devices, as sealant and as lubricant.

The use of PDMS in chemical microsystems emerged in the mid 1990s, when Xia & Whitesides introduced the concept of 'Soft-Lithography' as a micro/nano patterning method based on a molded PDMS stamp [88-89]. Just a few years later, the same replica molded PDMS stamps started a revolution in microfluidics, when Duffy & Whitesides described the plasma bonding of PDMS-PDMS and PDMS-glass [25]. By this, the full fabrication process of microfluidic devices was established, using relatively cheap and simple means (Figure 3.5). After a master is made photolithographically (typically a single layer of SU-8 on a Si-wafer, which is also the most basic lithography step possible), the remaining process is easily accomplishable in every chemistry lab. PDMS is mixed from two components, degassed to remove air bubbles and casted onto the master simply by pouring. After curing in an oven, a rubbery PDMS slab can be peeled off from the surface treated master. Since the material is soft, fluidic interfaces can be easily punched out with hollow punch tools made from syringe needles. Finally the slab, and another piece of PDMS or glass, are treated with an oxygen plasma (a low-cost plasma cleaner is sufficient) and bonded, by simply pushing them together. This procedure was quickly adopted by many labs, and PDMS became the dominant polymer material in the field of microfluidics research, with several hundreds of publications produced each year [50, 69].

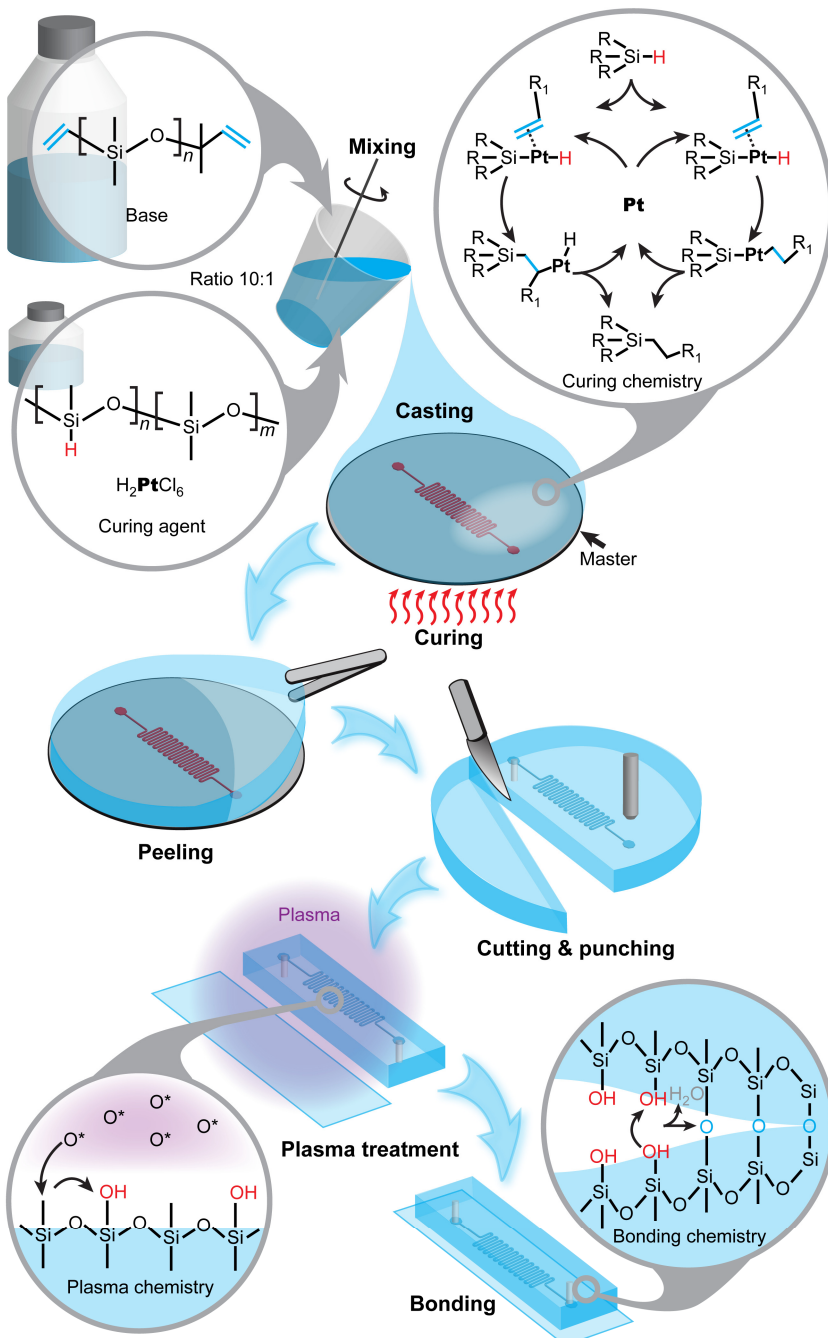


Figure 3.5. Fabrication of PDMS microfluidic devices, with chemistry of curing [90-91] and bonding.

In addition to facile fabrication, several other favorable properties of PDMS have contributed to this success. Most important is the optical transparency with low auto-fluorescence, which allows these devices to be used in microscopy - one of the easiest means of detection and visualization. PDMS also has good biocompatibility, as it is non-toxic and gas permeable. Not less important is the elasticity, which contributes to fabrication but also to reliable interfacing, since a tight seal is formed when supply and control tubing is pressed into the punched out conduits. PDMS elasticity is also the foundation of the simple, but powerful valve concept invented by Unger & Quake [81]. Lately, mechanics and microfluidics have been combined to create soft-actuators and robotics [92].

Disadvantages of PDMS are low solvent compatibility [93], in some cases also deformability, as it introduces compliance (Paper III) and non-linear resistance. In some applications, another limiting factor is the unstable surface chemistry after oxygen bonding, which gradually returns from the hydrophilic ($\sim 5^\circ$) to the hydrophobic state(109°) [94-95]. From the manufacturing point of view, 30min-1h curing time is much longer than the injection molding cycle, which can be completed within seconds. Regardless of these few shortcomings, PDMS, with its well-established prototyping schemes, is most likely to remain for years to come an important material in this field. All microfluidic devices described in this thesis were fabricated from PDMS, using soft-lithography.

3.2 MICROSCOPY

Just as the well known idiom states, “*Seeing is believing*”. When working with small structures and objects, microscopy is an essential tool. It makes visible microscopic features, which cannot unassisted be resolved by the human eye. The work presented in this thesis has been tightly intertwined with the use of microscopes, starting from the simplest inspection of microstructures to sensitive quantitative measurements of single cell chemistry. One can go even further and state that all microfluidic instruments and devices presented in this thesis can be considered to be tools or accessories for biological microscopy.

The history of optical microscopy dates back to the 16th century, where Dutch spectacle-makers Hans and Zacharias Janssen assembled the first compound microscope [96]. The next, and even more important milestones were set by Robert Hooke and Antonie van Leeuwenhoek, who used simple microscopes to describe for the first time the small-scale world, and introduced this technique to the biological society [97]. This was followed by a long list of inventions, including Köhler’s homogeneous illumination mode in 1893, Zernike’s phase contrast [98] and Nomarski’s differential interference contrast [99] methods, which improved imaging of transparent samples, such as cells. However, for molecular and cell biology the biggest breakthrough came with the development of fluorescence microscopy, which with its multitude of variations allows high resolution imaging of sub-cellular components. Fluorescence techniques now have the sensitivity to visualize single molecules, and makes quantitative characterization of chemical composition, reaction rates, diffusion and more, possible. Fluorescence microscopy techniques have been used extensively in this work to characterize the fluidic circuits and the kinetics of cellular chemistry.

Fluorescence microscopy techniques are used for visualizing fluorescent molecules, which are characterized by absorption and subsequent re-emission of light, where the emitted photon has a longer wavelength (lower energy) than the absorbed. The energy difference is dissipated as heat. This phenomenon is best explained with the help of the Jablonski diagram [100] (Figure 3.6 B). While fluorescence phenomena were already observed in the 16th century, and the name “fluorescence” was coined in the mid 19th century by G. G. Stokes [101] (the same Stokes who developed hydrodynamics) its use in biological microscopy emerged not before the beginning of the 20th century (Carl Zeiss’ UV microscope in 1904 and Oskar Heimstädt’s first successful fluorescence microscope in 1911) [96]. A rapid development phase followed, and by the 1930th various producers and commercial ultraviolet microscopes were already on the market. Another important contribution to fluorescence microscopy was brought about by the emergence of synthetic dyes in the mid 19th century [102]. In 1871, Adolf von Bayer created the first fluorescent dye, fluorescein, soon followed by many others [96] (e.g. rhodamine B by Ceresole in 1887). For the biologist, the true power of fluorescent dyes arose from the possibility to couple them to biomolecules, most notably to antibodies (Albert Coons, 1941) [103], allowing

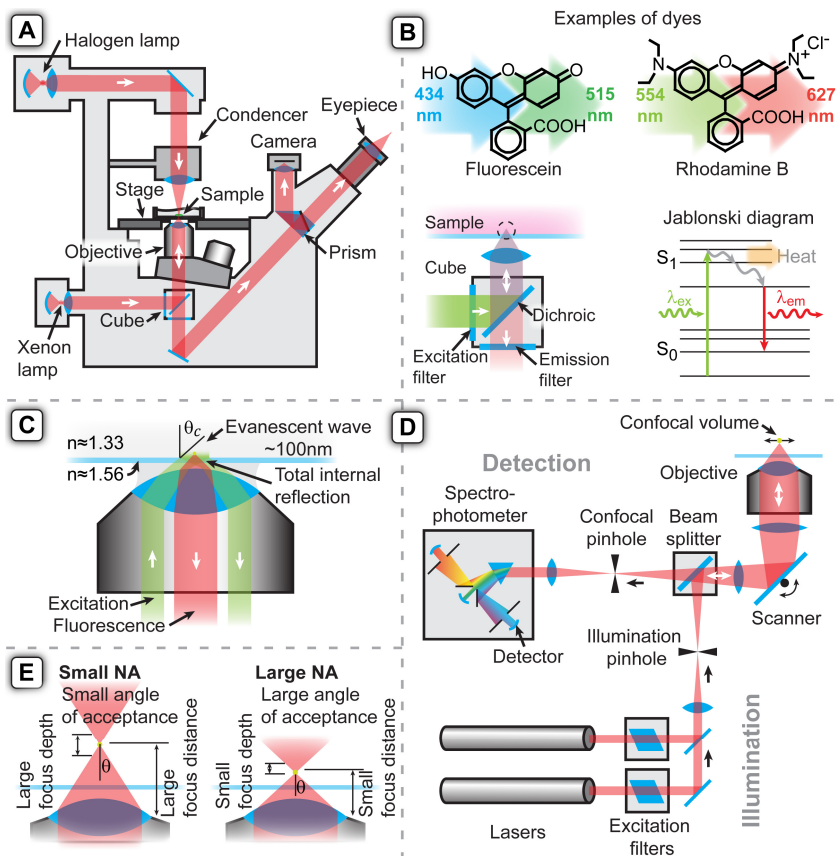


Figure 3.6. Essentials of optical microscopy. **(A)** Schematics of a common inverted epifluorescence microscope. **(B)** Principles of fluorescence microscopy and examples of fluorophores (dyes) [108-109]. **(C)** Principles of total internal reflection fluorescence (TIRF) microscopy. **(D)** Schematics of a scanning confocal microscope. **(E)** Choosing the objective – the meaning of numerical aperture (NA).

them to be used for highly selective staining of molecular components of cells. A large contribution to the current widespread use of fluorescent microscopes came from the invention of dichromatic mirrors (Johan Sebastiaan Ploem, 1967). By this point, fluorescence microscopy has developed into many branches, making use of specific molecular and spectroscopic phenomena. Examples are: fluorescence correlation spectroscopy (FCS) [104] & fluorescence recovery after photobleaching (FRAP) [105], allowing to study reactions and molecular transport; Förster resonance energy transfer (FRET) [106], which can elucidate structures of molecular assemblies, dyes whose fluorescence is altered by binding to other chemical species and can be used to study cell physiology, two-photon excitation [107] etc.

The principle of the fluorescence microscope (Figure 3.6 A-B) is to illuminate the sample with light at the excitation wavelength of a fluorophore or dye, while collecting at the emission wavelength. The key component of the microscope is a filtering system called **beam splitter**, which in most microscopes contains three parts: the **dichroic** mirror and two band pass filters for excitation and emission. The function of the dichroic mirror is to be reflective to a certain wavelength range, and transmissive to another. This allows separation of the excitation light, which is focused through the objective onto the sample, from the emission light, which emanates from the excited sample. Since different dyes have different excitation and emission spectra, filters and dichroics need to be exchanged to match the fluorophore. Therefore, for the convenience of use, filters and mirror are usually combined into small assemblies commonly called a “**cube**”.

Total internal reflection fluorescence (TIRF) microscopy is a modification of common fluorescence microscopy in order to image a very thin layer on a surface (Figure 3.6 C). This technique, invented by Daniel Axelrod in 1981 [110], is based on total internal reflection of light occurring at the interface of two media with different optical densities (n). When a beam, transitioning from a higher to lower refractive index material, hitting the interface at an angle which is larger than a critical angle θ_c (Eq 3.1), all light is reflected back. However, this reflection occurs in a finite layer near the surface, where the electromagnetic field reaches somewhat into the medium of lower refractive index. This **evanescent wave** is confined in a thin layer, about 100nm in thickness, which decays exponentially with distance from the surface [111]. Using the evanescent wave for exciting molecules confines the illumination to the nm scale layer. This eliminates background fluorescence, which would otherwise complicate sensitive measurements, of particular use, when imaging single molecules.

$$\theta_c = \arcsin \frac{n_{low}}{n_{high}} \quad (3.1)$$

In a typical example, the refractive index of glass is about 1.56, that of water is 1.33, giving a critical angle of 58°. In this work, we have used TIRF to characterize solution exchange near surfaces, in order to mimic the flow around adherent cells, while eliminating responses from higher layers. This was necessary, since faster solution exchange higher above the surface could give incorrectly shorter values for the exchange times (Paper III).

Confocal laser scanning microscopy (CLSM) is another technique based on fluorescence microscopy with high vertical (axial) resolution (Figure 3.6 D). The principle of confocal microscopy was patented by Marvin Minsky in 1957 [112]. Compared to wide-field fluorescent microscopes, which illuminate and accept light from various focal planes of the sample, confocal microscopes exploit small pinholes, which defines a sharp focus point, while illumination intensity and acceptance of light from outside the focal plane drop rapidly. While the simplest configuration of the confocal microscope allows collection of light from just a single point (point confocal), all modern confocal microscopes contain a scanning mechanism. The scanning action

is typically based on deflected mirrors, which sweeps the focus point in the xy plane. The light intensities collected from each point are then reconstructed into an image. If the focus point is also scanned vertically (z-axis), three dimensional images can be created. Modern commercial confocal microscopes integrate additional advanced optical instrumentation. Tunable excitation filters (AOTF) allow to adjust the power of the different excitation lasers. The dichroic mirrors can be replaced by an acousto-optic beam splitter (AOBS), which similarly use the interference principle to separate wavelengths to be reflected or transmitted. Instead of fixed thin film coatings, a layered structure is effectively formed when high frequency sound waves are compressing and expanding a piece of glass, changing locally its refractive index (interaction of phonons and photons). The great advantage of the AOBS is that all filtering properties can be instantaneously and electronically changed by synthesizing an appropriate signal for the piezoelectric transducer, which excites the glass. The processing of the emission light can be handled similarly, where tunable spectrometers can isolate multiple wavelength ranges, which can be simultaneously collected with highly sensitive sensors, typically photomultiplier tubes (PMT) or avalanche photodiodes (APD). This flexibility has made confocal microscopes indispensable for biologists. A multitude of fluorophores can be monitored simultaneously, helping to elucidate intracellular structures and phenomena.

Fluorophores (dyes) are molecules with fluorescent properties. However, modern fluorophores have more advanced duties than simple shining. They can be conjugated to molecules such as antibodies and lipids, which can bind to particular biomolecules and cell components, allowing them to be visualized. Another important type of fluorescent dyes are those which change their fluorescent properties after a particular modification, or environmental change. For example, temperature dependant fluorescence (e.g. Rhodamine B [113], molecular beacons [114]) can be utilized for temperature measurements. The fluorescence of some dyes, such as Calcium Green™ [115], Fluo-3, or Fluo-4 [116], increases upon binding to Ca^{2+} , one of the most important regulators of cellular processes. Therefore, these dyes allow physiological monitoring of calcium levels within cells. YO-PRO-1™, another example, displays similar fluorescence changes when binding to DNA [117]. Other dyes need modifications in their molecular structure to become fluorescent. For example, fluorescein diphosphate (FDP) becomes fluorescent when its phosphate groups are removed by alkaline phosphatases. Therefore it can be used to monitor enzyme activity in cells [118]. The portfolio of methods used in cell biology has been redefined by fluorescent proteins, first green (GFP) [119], and now also many other colors. GFP genes can be inserted in particular places of the genome, and the resulting fusion can reveal the expression of otherwise invisible proteins. Another important aspect of all fluorophores is the chemical and photo stability. Many classical fluorescent dyes, in particular fluorescein, are prone to degradation (photobleaching) due to the excitation light. A large selection of advanced dyes, featuring superior photostability, high fluorescence quantum yield, and a wide range of excitation wavelengths, is available today. Further developments concern the engineering of interactions of dyes with biological matter, such as specific transport across the

boundary of cells or organelles, and deposition in selected locations. This allow for accumulating them inside cells (e.g. acetoxyethyl ester conjugates [Paper III & IV]) or their use for probing ion-channel function (e.g. YO-PRO-1 passing through TRPV1 channels [Paper II & VII]). Thus, fluorophores provide biological microscopy with a great advantage - processes inside living cells can be followed under physiological conditions in real-time with very high spatial and temporal resolution. However, caution has to be taken, as electronically excited dyes in cells are reactive molecules. They may also pose unwanted side-effects on cellular processes. And establishing a fluorescent probing scheme for a new experiment can be a serious challenge.

Limits of microscopy. Resolution of optical imaging techniques has fundamental limits caused by the diffraction of light. This diffraction limit was studied by Ernst Karl Abbe 1873, who found that light cannot be focused to an infinitely sharp spot, but to a minimum spot size d , as defined by eq. 3.2 (known as **Abbe diffraction limit**).

$$d = \frac{\lambda}{2NA} \quad (3.2)$$

where λ is the wavelength of the light and $NA = n \sin(\theta)$ is the numerical aperture, describing the capacity of the optical system to collect light. n is the refractive index of the working medium and θ is the maximum acceptance angle as shown on figure 3.6 E. The larger the maximum angle of acceptance, the higher the NA , and the better the resolution. However, a high NA has another advantage, the collection of a larger fraction of photons of fluorescence, which are emitted equally in all directions (Table 3.2). Difficulties with high NA objectives are a shallower depth of focus and shorter focal (working) distance. High NA (>1) objectives require an immersion liquid (water, glycerol or oil), otherwise the portion of light coming in at a high angle could never leave the sample, due to the total internal reflection in the cover slip. Therefore the NA of the optical system cannot be larger than the smallest refractive index present in the medium separating sample and objective. Air objectives therefore have a $NA < 1$. Last, but not least, manufacturing lenses which can focus light equally at a larger range of angles requires higher precision and quality, resulting in a high price tag on high NA objectives. (For example, 40x microscope objectives with 0.65 and 1.3 NA cost about 7'000 and 50'000 kr respectively. [120])

Table 3.2. Illustration of light harvesting efficiencies of objectives with different NAs, working with an aqueous sample ($n = 1.33$). For isotropic fluorescence, the fraction of light collected by the cone of acceptance would be $(1 - \cos(\theta))/2$.

NA	$\theta(^{\circ})$	% of light collected
0.8	13	1.3
0.7	32	7.6
1.3	78	35

3.3 SIMULATIONS

As discussed before, many physical processes are described by partial differential equation (PDE) systems, like the Navier-Stokes (Eq. 2.18) or convection-diffusion (Eq. 2.27) equations, which are describing fluid flow and transport of chemicals. Unfortunately, solving these equations is often challenging, even in case of extremely simple geometries, and is completely impossible in almost all real-life settings, where multiple physical phenomena, different materials and objects with complex shapes are combined. This problem has been greatly alleviated by the emergence of simulation methods, which together with the rapidly developing high power personal computers, have become commonplace in all branches of engineering.

To make computer representations of PDEs describing spatially and temporally continuous physical fields (e.g. pressure, temperature, concentration etc.), these fields have to be discretized by slicing space and time into finite numbers of elements, which is represented by the name **finite element method (FEM)**. In contrast, a continuum, can be thought of as made from an infinite number of elements. All values themselves can only be represented with limited precision. (e.g. the 64-bit double precision floating point data type can hold values from about $\pm 10^{-300}$ to $\pm 10^{+300}$, with a precision of 15 decimal points. It sounds like an enormous range and precision, but when small and big numbers are added and subtracted from each other, the rounding errors can lead easily to numerical chaos). After dividing the complex object into small, simple shapes, which can be described by algebraic equations, these elements are joined into a network, called **mesh**, with connected nodes. Some values in some nodes will be defined by boundary conditions, others will be unknown. In a similar way, as described in section 2.2.2 for pressures and flows in microfluidic channel networks, all relations between the mesh nodes can be encompassed into large algebraic equation systems. Solving the equation systems with the help of matrix algebra gives the unknown values in each mesh node (simulation results).

Modern finite element software packages have become convenient tools with easy graphical user interfaces, allowing engineers and scientists from various disciplines to perform simulations, while requiring neither any programming skill nor understanding of the complex mathematics behind the solver algorithms. Nevertheless, it is essential that the user knows the system and physics behind it, otherwise resulting graphs may look beautiful, but have little touch with reality.

The typical workflow of finite element modeling is depicted in figure 3.7, using a microfluidic mixer as an example. The first essential step is to split the system into parts and eliminate unimportant details and those parts which can be calculated analytically. This matters greatly, since the total number of elements in the model is finite and limited by the available working memory. A well chosen simulation region allocates computation resources to the regions in the geometry where they are needed. For example, the flow rates in the supply channels of the microfluidic mixer can be calculated using analytical expressions (Table 2.1), therefore the interesting region is only around the point where the two flows meet. Thereafter the geometry of the

selected part of the device is drawn, followed by assigning the physics (e.g. Stoke's equation and convection-diffusion equation), materials properties and the relations between all these phenomena. In the example, the convection-diffusion depends on the flow velocities calculated from Stoke's equation, but it can also have the opposite relation if the fluid viscosity depends on the substrate concentration. Determining these relations properly is an essential part of model building. Failing to do it, can waste computation power or result in errors. Proper boundary conditions must be selected and finally, the geometry should be meshed into a network of finite elements. Even though the mesh is a purely computational construct, creating it requires physical consideration. As the mesh discretely samples the continuum space, its density has to correspond to the variations, such that the regions with rapid change have the highest, while the more homogenous parts can have a lower density. The mesh density has to be finer than the size of the features it tries to reveal. This is analogous to the Nyquists-Shannon theorem for signal sampling. Once an actual simulation succeeds, the results have to be verified - are they physical and realistic? For example, are inflow and outflow of liquids equal, is total amount of substance conserved, or how do simulations correspond to experiences from experiments? If profiles, which are expected to be smooth, oscillate, the reason is most likely a numerical instability - the consequence of poor meshing. In general, a good mesh has been achieved when further increase of its density does not change the results significantly (convergence).

The use of simulations can serve two purposes - to understand nuances and mechanisms in experiments, which are hard to measure directly, or to evaluate the performance of device designs before fabricating them. This saves significant time and resources. In the presented work, the FEM modeling package COMSOL (Founded 1986 by students of the Royal Institute of Technology in Stockholm) has been used extensively for both purposes [63].

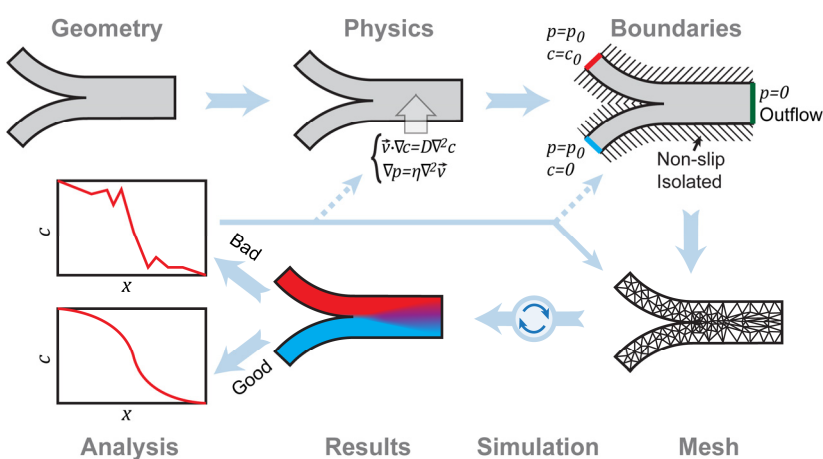
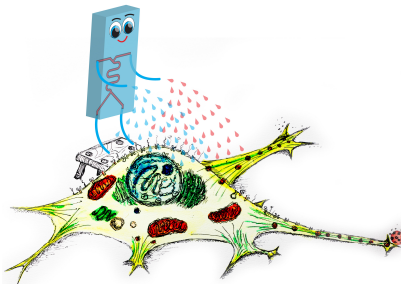


Figure 3.7. A typical process of finite element modeling.

4. TECHNOLOGY



For a living organism to function, constant exchange of information is required on the cellular level, where the messengers are different chemicals. In order to study the machinery of the cell, it is important to be able to control and adjust its surroundings. The central theme of this work is the development of advanced tools to handle chemical environments at the size scales of the cell with the help of microfluidic technology.

4.1 MICROFLUIDIC DILUTION

The preparation of mixtures and dilutions is a common experimental procedure in most areas of chemistry and molecular biology. Since a significant amount of research involves optimization of concentrations and mixing of reagents by trial and error, automation is very desirable. The use of a microfluidic format for mixing gives additional benefits, such as low reagent consumption and low device cost, as compared to liquid handling robots. In the following chapter a number of microfluidic mixing concepts are presented and compared.

In principle, dilutions in microfluidics require the same steps as in a macro-scale lab, metering reagents and mixing them. If the required dilution factor is large, it is usually not practical to dilute in a single step, but rather in several steps, starting from a concentrated stock solution (Figure 4.1).

Metering is the most crucial step, as it determines the accuracy of the final concentration. In microfluidics, various principles exist to determine the ratios of supplied fluids. Metering can be based on a ratio of input flows, or it can be defined by known volumes of reservoirs. Figure 4.1 depicts four of these concepts. In the first example, the mixing ratio in a continuous flow device is set by the ratio of external pumping rates (e.g. syringe pumps), by the ratio of pressures on liquid reservoirs, or by hard-wired differences in fluidic resistance of the channels. These diluters can be sequentially combined into networks in order to generate spatial gradients, whose shapes are controlled by the inflows [121]. Such gradients were, for example, used to dynamically regulate the nutrient levels of yeast and elucidate its metabolic regulation mechanisms [122]. The second type is also based on the ratio of flow rates, but here

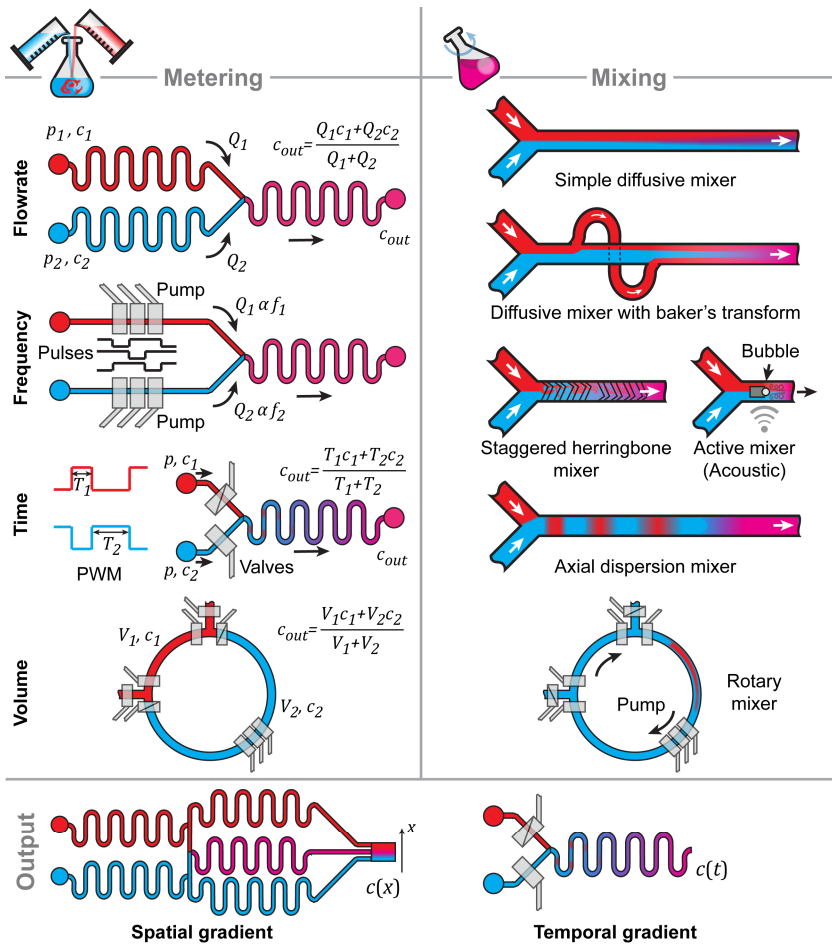


Figure 4.1. Generation of dilutions in microfluidics.

the flows are generated by on-chip peristaltic pumps, which are controlled by a pneumatic pulse sequence, whose frequency is proportional to the flow [123].

Peristaltic metering can be also used for volumetric injections. In this case the number of cycles is more important than the frequency [124]. In the third method the concentration is equally controlled by flow rate, but in a time averaging way, where the contributions are determined by the length of flow pulses emerging from supply channels. Concentration control with variable pulse lengths is the fluidic counterpart to pulse width modulation (PWM), commonly used in electronics to convert digital codes into analog signals [18] (Paper I & II). In the fourth example, the metering is based on the volume of defined channel segment [125-126].

An important analytical figure of merit is, of course, precision, where many factors can contribute to the practical results. If we put aside possible clogging by dirt particles etc. (gross error), then there are two major contributions, the precision of the chip and the precision of the control signal. In microfabricated devices, the channel length is normally much larger than the width, and all fabrication techniques allow it to be produced with negligible variance. Much harder is to control the uniformity of the channel cross-section, in particular height. Neither spin-coating nor etching produce exactly uniform structures. Thick (30 μ m) SU8 has about ~10% or more height variation, [127], glass etching [128] and DRIE [42] about ~5%, and SOI wafers [43] ~1%. Size variation can have different effects on precision (Table 4.1). For example, the hydrodynamic resistance depends on the 4-th power of the cross-sectional size (Table 2.1), while the volume only on the 2-nd, which means that pressure driven metering (flow rate based and PWM) is twice as sensitive to geometry variations compared to the channel volume-based ones (peristaltic pumping and reservoirs). Higher precisions in the control signals are typically easier to achieve. Typical electronic pressure regulators have an accuracy of ~1% [129]. Peristaltic and PWM metering relies on timing precision, which is easily achieved with electronic control, but since they involve also pneumatic actuation by solenoid valves, which requires a switching time of a few to 10 ms, the maximum frequency becomes limited.

Mixing is the next step in making dilutions. Mixing speed and efficiency determine time response and stability of the diluter. It is desirable to have a precisely determined output concentration with no spatial or temporal variations. The simplest mixer is the T-junction, where two flows meet and co-flow until molecular diffusion eradicates the concentration differences. Since there are no turbulences, this processes is slow. It can be boosted by increasing the contact area, where liquid sheets are pressed wider and thinner. The contact area can be increased even more efficiently by using the so called baker's transform (due to the dough making analogy), where a fluid stream is split and rejoined such that opposite sides will be connected. The problem with the baker's transform circuits is that they require either crossing channels (multilayered design) or 3D channel geometries [27, 130]. Both are complicated to achieve with most of the common fabrication methods. While in intermediate Re number flows mixing eddies can be generated by various bumps and sharp edges, passive stirring at low Re is more challenging [131]. An elegant solution is a staggered herringbone mixer (invented by Stroock & Whitesides, 2002), where small diagonal grooves at the bottom of the channel guide the liquid and give its flow field a non-zero component in the y-z plane (Eq. 2.24). This leads to general rotation, which can efficiently mix substrates in about 1cm of the channel length [132]. Some other micro-stirring concepts introduce radial velocities by electric fields or sonication. An interesting example is an acoustic micromixer using a trapped bubble, which can achieve complete mixing in a few milliseconds [133]. Pulsed flows, like the one produced by PWM flow metering, are favorable, since flow segmentation together with Taylor dispersion helps to improve mixing efficiency (Paper I). A similar process happens also in rotary mixers, where one pulse is circularly pumped in the channel, where it spreads due to the Taylor dispersion [124-125].

The choice of the mixing concept depends on the required features. Should there be a continuous outflow, or should the mixtures be made in portions? What are the required response time, precision and dynamic range? Can it be made in one stage, or need multiple diluters be connected in series? Shall the output be a spatial or temporal gradient? Compromises are generally needed and a higher dynamic range and precision requires longer preparation (response) time (Table 4.1).

Table 4.1. Comparison of dilution concepts in microfluidics.

	Flow rate	Peristaltic	PWM	Volume (reservoirs)
Continuous outflow	Yes	Yes	Yes	No
Geometry dependence	$\propto r^4$	$\propto r^2$	$\propto r^4$	$\propto r^2$
Continuously adjustable output	Yes, Pressures	Yes, Frequency	Yes, Pulse length	No, Discrete steps
Output	Proportional	Proportional	Proportional	Exponential # of dilutions
Increasing dynamic range	Multiple stages	Multiple stages	Multiple stages	-

4.2 LOCALIZED DELIVERY OF CHEMICALS

4.2.1 HYDRODYNAMIC FLOW CONFINEMENT

In a stereotypic view, microfluidic devices are confined laboratories on chips, into which materials and samples are introduced, and all the magic of the experiment occurs inside channels surrounded by walls. Instead, this work describes another, younger and less explored paradigm in microfluidics, where useful properties of micro-scale fluid flows are projected beyond the boundaries of the device, into an open volume. This allows for easy integration with existing instrumentation and experimental environments, and lowers the acceptance barrier for the new technology.

One of the useful properties of microflows is their stability, which has allowed to develop devices to address biological cells with high spatial [11] and temporal [134] resolution. To use this feature, the cells have to be brought or even grown inside the devices, which can be unfavorable. For example, adherent cells or cells extracted from tissues lose their spatial organization when suspended. Free-floating cells in suspensions may also increase the risks of clogging of smaller channels. The alternative approach of culturing cells inside the device can be challenging too, due to different rates of oxygen and nutrient transport, requiring additional optimization.

Most of these concerns can be alleviated by separating cells and fluidics. Biologists can prepare their cell cultures and tissue slices in conventional Petri dishes, using well established protocols, and the fluidic functions can be brought in when and where needed. The simplest device of this kind is a glass capillary injecting a liquid. Though widely used, its capacity to define the exposed area is very limited due to diffusion. As described before (Ch 2.1.2), microfluidics offers means to combat diffusion by convective flow and therefore allows to maintain inhomogeneous concentration distributions. This principle is not limited to closed channels. If fluid leaves into the open volume, it can be captured and circulated back into the device by sufficient neighboring inflow. Such circulation forms a small reservoir, whose boundaries are defined by hydrodynamic flow-lines and the content by the outflow. In the following we call this circulation a **hydrodynamically confined flow (HCF)**.

The general concept of using simultaneous out- and inflows (circulation) in liquid delivery is not new, it has in several incarnations found use in different devices (Figure 4.2). One of the earliest is the **push-pull cannulae** (developed by J. H. Gaddum, 1961) [135], used to sample neurotransmitters in brain. This early device suffered from the risk of damaging the tissue by the liquid, got frequently clogged and became contaminated by cells and blood. An improvement, the dialytrode (by Delgado et al, 1972) [136], was introduced, separating the liquid flow from the cells by a semi-permeable polysulfone membrane. The chemitrode, a similar probe, was reported around the same time [137]. The practical construction and efficiency of this sampling device was improved by U. Ungerstedt (Karolinska Institute) in 1974, using a hollow membrane tube [138]. This method, known as **microdialysis**, has become widely used to sample neurochemicals in both research [139] and clinical settings [140]. Although related, microdialysis is not using hydrodynamic confinement, since the flow is separated from the external volume by the membrane, and coupling occurs only by diffusion.

In 1996, semi-open volume confinement of liquid has been patented by Mitsumori et al. for a wet cleaning nozzle, invented for processing of large substrates of the kind used for solar cells and LCD displays [141]. Confinement occurs on a dry surface, where a precise flow balance allows to avoid leaks from the close gap between substrate and flow chamber, such that it required no seal or mechanical connection. This device is a gigantic, several orders of magnitude larger relative of the HCF systems discussed in this thesis. In a same year, another microscopic flow confinement system emerged, used as a **fast local superfusion** technique for the stimulation of adherent neurons [142]. Here, two glass capillaries (\varnothing about 10 μm) are positioned in close vicinity (~20 μm) around the cell, one used for injection, the other for aspiration. This setup formed a HCF about 30 μm in size, and pressure switching allowed solution exchange on the ms time scales. This tool has been an essential component in studies of the motility of dendric filopodia [143], and potentiation of synapses [144]. However, it suffered from many practical shortcomings. It was hard to control the exact geometries of the capillaries, which affected the flowrates. It was also tedious to position them repeatedly, since already slight variations in distance can cause a significant change in the flow field and exposure profile. The aspect of

positioning has been simplified by combining two needles into one coaxial superfusion pipette (**Picoliter fountain-pen**) [145], where a smaller injection pipette is placed through the orifice of another, the larger one, for aspiration. Even though it reduced the positioning difficulties of two separate pipettes, it introduced much more complex assembly and interfacing requirements. Somewhat simpler to handle is the dual pipette pulled from the theta-tube [146]. An important limitation of both of these dual-capillary systems is that they do not allow fast exchange of perfusion solution. As with all glass pipettes, they also are extremely fragile, making their handling cumbersome. In any case, dual-pipettes have made an important contribution to research, where they have been used, for example, to stimulate artificial neural networks [147] and measure signal propagation in them [148], as well as for stimulation of cardiac myocytes [149] and collection of mRNA [146].

Most of the problems associated with glass pipettes can be overcome by using microtechnology, which allows repeated fabrication of channels with well defined geometries and positions, as well as to design circuits that allow fast solution exchange, dilution and other liquid processing functions.

First microfabricated HCF device was the **Microfluidic probe** (by D. Juncker & E. Delamarche in 2005) which has been inspired by inkjet and spotting technologies, but was crafted to provide superior spot-quality for surface processing in liquid environments [150-151]. This device resembles a print head, brought into close vicinity of the surface such that the channels point towards it. The first practical difficulty associated with this design was the alignment of the large head, which has to be parallel to the surface in order to avoid contact and damage, and close enough to it to deliver solutions. Another shortcoming was the rather complicated fabrication, which consisted of three lithography steps, HF etching, two DRIE processes, dicing and bonding. These aspects were somewhat improved in a later vertical design by the same inventors [152-153]. The microfluidic probe was used to pick up cells, pattern antibodies [150], and stain adherent cells and tissues [150, 153-154]. From a biologist's perspective, many practical limits remained, such as the apex, which covers the processed area and restrains the use of upright microscopes and limits access by other probes such as glass pipettes, microelectrodes or optical fibers, used in various biological experiments. These restrictions are particularly severe for neuroscientists, who would like to combine solution exchange with electrophysiological recordings.

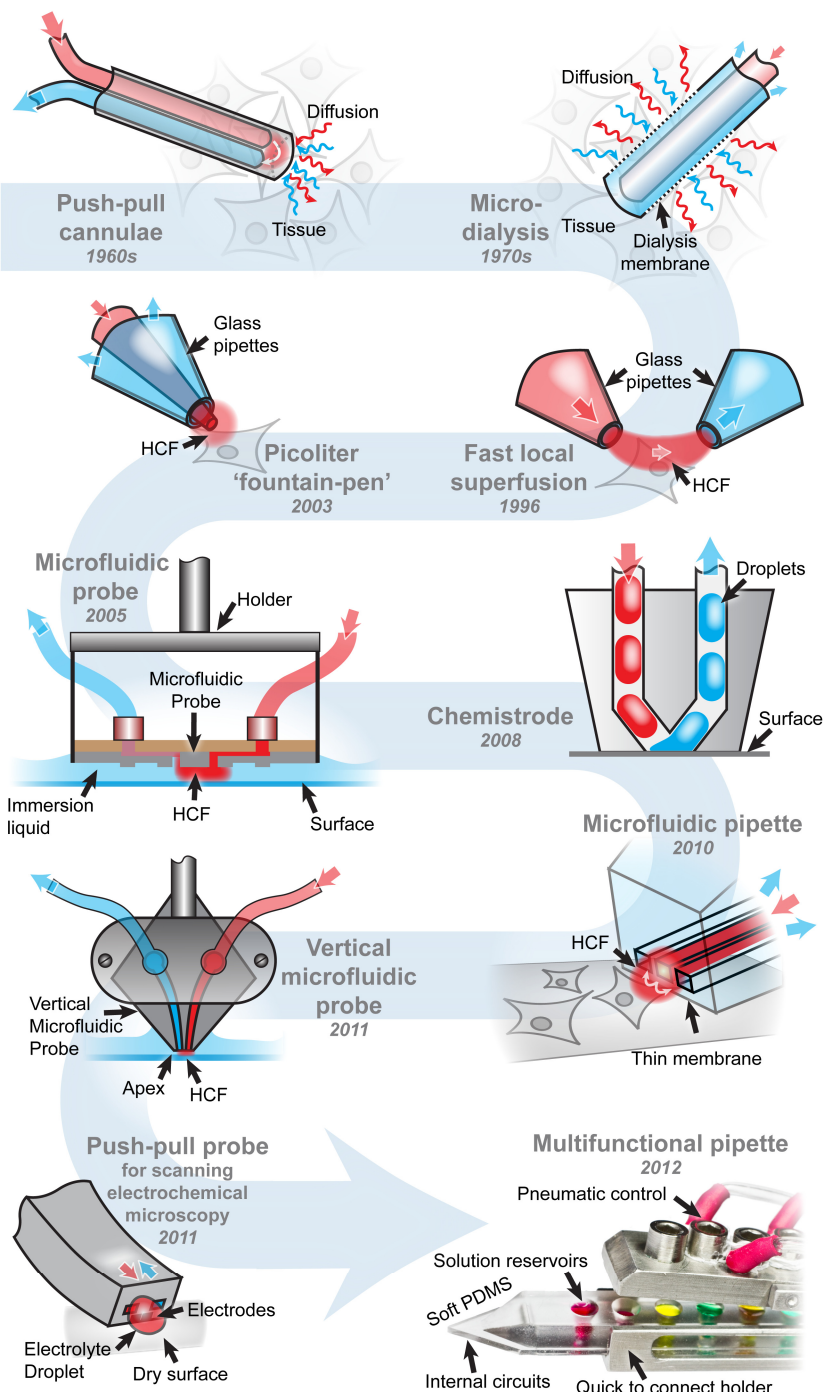


Figure 4.2. History and examples of hydrodynamically confined flow devices and related concepts.

Table 4.2. Comparison of microfluidic probes and multifunctional pipette.

Features	Microfluidic probes	Multifunctional pipette
Alignment	Apex parallel to surface	Variable application angle
Angle sensitivity	Sensitive around 2 axes Large (mm scale) apex would collide with surface	Inensitive Application angle flexible Low sensitivity to rotation around tip axis due to sharp tip
Vertical height sensitivity		Identical
Confinement boundary	Sharper	Smoother
Shear stress on the sample	Higher	Lower
Microscope compatibility		
- Inverted	Yes	Yes
- Upright	No	Yes
- Transmission	No	Yes
Compatibility with additional probes	No	Yes
Solution exchange	No	Yes (4 solutions ~ 50 - 100ms)
1D gradients	Yes	Yes
2D gradients	Yes	No
Chemical compatibility	High	Limited to aqueous solutions
Supply	External through tubing (cleaning needed)	Integrated wells (cleaning not needed)
Flow driving	Syringe pumps	Air pressure from computer controlled pneumatics
Materials	hard Si/glass (mostly)	Soft (PDMS) Simple
Fabrication	Complex Multistep photolithography	One step soft-lithography. Most limiting step is individual tip punching
Fabrication infrastructure requirements	High	Low
Device usage	Most likely multiple use	Most likely disposable use
Optimal for	Chemical surface processing	Single-cell manipulations

We, initially unaware of the microfluidic probe, were driven to build our **Pipette** by the need of biologists and biophysicists to exchange the solution environment around cells (superfusion), to stimulate them or to create gradients in order to drive membrane migration. Knowing that glass pipettes are widely used for these purposes, we saw our device as a modern variant of the classical pipette with extended functionality and more convenient use - and named it multifunctional pipette. In contrast to the microfluidic probe, it is applied under an angle, just like glass needles in typical biological experiments. The combination with other probes, e.g., electrophysiological recording pipettes, and upright microscopes, remains unrestricted. Our device works well in conjunction with micromanipulators, and needs no specific station to position and align it [155]. Furthermore, as biological experiments can require series of multiple reagents to be applied to a cell, our device has the functionality to switch solutions and create dilution series through a single HCF. In order to perform switching, no physical movement of probe or sample is required, another advantage for the biologists, since motion could hinder the use of other probes or even disturb sensitive imaging or recording.

Other, related devices exist. For example, the **Chemistrode** (not to be confused with the aforementioned Chemitrode, which is a different concept) by Chen & Ismagilov [156], is used for both stimulating and collecting responses from local areas on a surface, using droplet microfluidics. This probe is not a HCF device, since conformal contact with the surface is required during operation. Very similar is also a PDMS spotter used for fabrication of protein chips [157], but instead of droplet flow, continuous flow was used there. Some other device are applied to deliver, maintain and refresh microscale droplets on dry surfaces. One example is a microfluidic probe, which used a hydrophobic-philic apex region to define the flow chamber [158]. A similar approach had been shown before, also for liquid guidance inside channels [159]. A different open volume push-pull probe was reported for the delivery of fresh electrolyte in scanning electrochemical microscopy [160-161].

It is interesting to note that chemical circulation is actually used in nature for the same purpose: to stimulate cells. Nature's probe is called **synapse** (more precisely chemical synapse), where one nerve cell stimulates the other by the release of neurotransmitters. In order to avoid contamination and to control the stimulation, neurotransmitters can be pumped back by transporter proteins [162]. Differently from the above described liquid handling devices, this circulation is not hydrodynamic but molecular, and occurs on significantly smaller size scales.

4.2.2 SOLUTION EXCHANGE - NEED FOR SPEED

As mentioned in the preface to this chapter (Ch. 4), all communication between cells is mediated by exchange of chemical species - ions, small and large molecules. In order to study this communication, we need tools, both for detecting and for

stimulating. The processes themselves can occur on various timescales: Pathways involving regulation of gene expression have slow response times (minutes to hours) [122, 163]. Neural communication, on the other hand, is fast - for example seeing or feeling something is separated from the perception in the brain by mere milliseconds, even though it requires multiple steps of cell-to-cell information exchange. Even higher, microsecond scale time resolution is needed for signals arriving from either ear to enable us to locate the origin of the sound (stereo effect) [163]. This is owed to the fast ion-channels in the membranes of nerve cells, which receive and carry signals.

Ligand-gated ion-channels in the synapse of a receiving cell are sensing to the release of neurotransmitters from another cell. Some of these receptors can have gating constants of only a few tens to hundreds of microseconds (e.g. Acetylcholine and AMPA receptors) [164-165]. Fortunately, as ion channels are conducting charged ions, electrical current through them can be relatively easily measured by the patch-clamp technique and high sensitivity amplifiers [166]. Using small membrane patches extracted from cells and immobilized at the tip of a glass pipette allows measurements of current, even through individual ion-channels (single-channel recording). In order to study kinetic and different steps of the gating process of these channels, it is also important to apply a stimulus, the chemical ligand, with time resolution higher than the opening and closing of the channel. This is not trivial and has been the subject of many studies. The performance of solution exchange is highly dependent on the instrumentation and the nature of the sample. The shortest solution-exchange times can be achieved by switching flows on the tip of a glass pipette (\sim 10-20 ms) [167], by steering the streams from a theta-tube (200 μ s) [168], or by using piezo driven scanning of fluid streams ($<$ 100 μ s) [165]. More complicated is the situation around cells, which can vary in size, and be either suspended on a pipette or adherent to a surface. For suspended cells, microfluidic open volume superfusion can produce exchange times of about \sim 30 ms [169]. With glass capillaries and special flow chambers, exchange time of \sim 10 ms were reported for small cells [170] and 200-400 ms for large *Xenopus* oocytes.

Solution exchange times have often been characterized by liquid junction potential measurements in the tip of glass pipettes, which represent well the settings of single-channel recordings, but not those of actual cells. V. Pidoplichko [171] characterized the relationship between sample size and solution-exchange times as nearly linear: \sim 0.8 ms per μ m of cell diameter. Theoretical models suggest that 20 μ s exchange times are possible for small patches [172].

Fast timescales can not only be found in gating of ion-channels, but also in other cellular processes. Some, such as electron-transfer processes or passage of ions through ion-channels [162] are much faster than the technically possible solution exchange times. More relevant are the timescales found in enzymatic reactions [173] and in conformational changes of large protein complexes, where characteristic time constants can easily be on the order of tens of milliseconds to several seconds [174].

4.2.3 OTHER METHODS TO DELIVER CHEMICALS

While hydrodynamic flow confinement is a relatively universal method to control the chemical environment at size scales in the area of 10-100 μm , other techniques exists, which can beat a HCF device in speed and size, but are more limited for specific applications.

Photolysis can be used to generate active molecules by optically releasing them from biologically inactive caged pre-cursors. As the method is extremely fast and localized ($<1 \mu\text{m}/<1 \mu\text{s}$) [175], it has gained popularity to stimulate neuronal networks, where the use of lasers and acousto-optic scanning allows to define spatial exposure patterns. This method has also its limitation, in particular the need for caged substances. Currently there are caged forms of acetylcholine, glutamate, calcium, GABA, glycine, and IP₃ available [176]. Control of the exact concentration, the inability to remove released substances by other means than diffusion, and the complex experimental setup are other difficulties.

Iontophoresis is analogous to pressure driven injection through capillaries, only that electrical current is used instead. A problem, this technique shares with other electrokinetic mechanisms is that transport mode is more substance-specific than the pressure driven counterpart [177]. **Organic ion pumps** [178] are somewhat similar to iontophoresis. Here, ion-conducting polymer materials are used to eject ions by means of current. A related technique is **nanopipette** based delivery [179], where electrical pulses are used to eject single-fluorescent molecules from a $\sim 100\text{nm}$ pipette tip in a scanning ion-conductance microscopy (SICM) setup.

Nanoliter patterns [180] based on two phase aqueous polymer solutions have been used to reduce diffusion and maintain the chemical composition in artifical cellular microenvironments. An advantage of this technique is that a large number of chemical environments can be created and maintained without continuous active intervention. It is, however, limited to experiments where a steady environments is sufficient, since the polymer hull around the cell does not support fast changes in composition.

Dip-Pen nanolithography (DPN) [181] is a surface patterning technique for features on the size scale of 1-100 nm, using an AFM tip. It cannot be used for maintaining liquid environment around cells. An enhancement of DPN is the **nanofountain probe** [182-183] featuring a molecular ink-feeding mechanism. **FluidFM** [184], is another variant of AFM, where the injection aperture is milled into the tip by using a focused ion beam. It can work as a regular AFM, but also penetrate the cell membrane and inject femtoliter amounts of liquids.

4.3 FUNCTIONAL BIOMEMBRANES

Biomebranes form the reaction vessels for the chemical machinery of life. Universally from small bacteria to human cells, they are confining all necessary components and nutrients [162]. Material and information transport can occur controllably and selectively through exo- and endocytosis, transmembrane proteins or sometimes just by diffusion. This vital role of membrane proteins in orchestrating cellular processes, has made them also essential drug targets. Up to 70% percent of new drugs address membrane proteins [185]. In a different aspect, biomembranes represent an intriguing physical structure: a molecularly thin two-dimensional fluid, where the motion of molecules is restricted in normal direction of the membrane, while they can easily diffuse laterally [186].

The role of biomembranes in the context of this thesis is significant, as all example applications of the developed devices directly addressed biomembranes, either by activating ion-channels, inducing membrane vesiculation, or by creating or manipulating artificially assembled model membrane structures on solid supports.

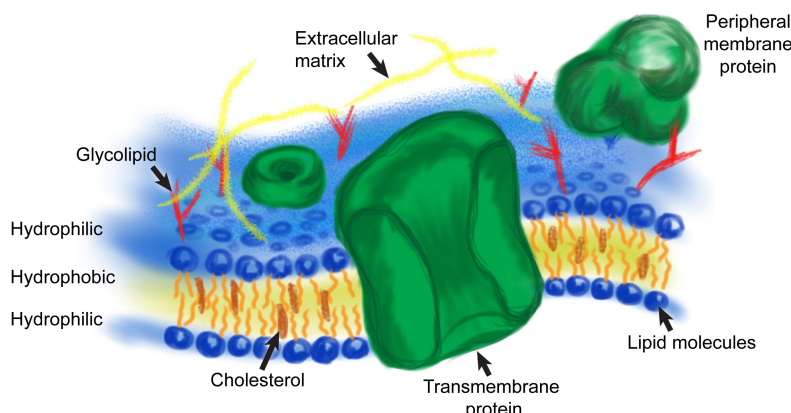


Figure 4.3. A cell membrane and its components

4.3.1 STRUCTURE OF THE BIOMEMBRANE

The biomembrane is a thin elastic sheet, self-assembled from various amphiphilic lipid molecules [187]. Lipids have a hydrophobic tail, which is most commonly composed of two fatty acid chains, a hydrophilic head which often consists of a phosphate moiety (phospholipid), and a small organic headgroup, such as choline. Both parts of the molecule are linked together by a glycerol unit. When brought into water, the lipids spontaneously line up their hydrophobic tails and assemble into thin

sheets, screening their nonpolar ends from the polar environment. The most efficient screening is obtained in an arrangement where two molecularly thin sheets of lipid film orient their hydrophobic sides towards each other, forming a bilayer. The film remains fluidic, as the molecules are not covalently interconnected, but held together by weak interactions [188]. Molecules other than lipids can populate the bilayer, either by dissolving into the hydrophobic inner part of the membrane (cholesterol and other sterols), by chemically conjugating to the lipid head group (sugars and small proteins, forming glycolipids and lipoproteins), or by embedding themselves into the membrane, often spanning it entirely. The last category is most important, since membrane-spanning proteins fulfill numerous transport, sensing, regulatory and other functions in the membrane [162]. With this diverse composition, the membrane is no longer a passive layer of mixed molecules, separating the inside from the outside of a cell, but rather a highly functional active boundary, which controls and regulates the concentration of molecules on either side, establishes identity, and manages the connection to neighboring cells.

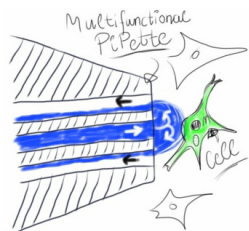
4.3.2 PROPERTIES OF THE BIOMEMBRANE

Major features of the biomembrane are elasticity and fluidity [189]. The elasticity provides the cell with the ability to adapt its shape to environmental cues, such as changes in temperature, osmotic pressure or other sources of stress. Fluidity, on the other hand, serves various transport and interaction needs. Self-healing after rupture [190], distribution of different lipids to other regions of the membrane, and the ability to fuse and mix molecules are some of the beneficial consequences of membrane fluidity [162]. Another major aspect is the need for insertion of lipids and proteins after their biosynthesis, which is also ensured by the high lateral mobility of the membrane. Finally, molecules can meet in the fluid lipid matrix, interact and generate chemical signals [162]. Other biomembrane properties are high electrical resistance and limited ion permeability, while gases, lipid-soluble molecules and small amounts of water can pass the boundary almost unrestricted [162]. Some of the beneficial properties, in particular the ability to host ion channels and other membrane proteins, have led to the desire to construct biomimetic membrane models [191]. In this context it is desired to maintain the fluidic features of the membrane, while managing to stabilize and immobilize the nanometer-thin assemblies. A practical solution to this problem is the solid-supported lipid membrane.

4.3.3 SUPPORTED LIPID MEMBRANE TECHNOLOGIES

In order to facilitate scientific studies and the technological use of biomembranes, a planar, fixed geometry is favorable [191]. Many probing techniques, microscopy, and patterning techniques such as photolithography are constructed for planar substrates.

Compatibility with these technologies has helped to investigate and exploit membrane features to a great extent. Supported lipid membranes can serve as biomimetic surface coating [192]. Moreover, selective transport can be investigated, for example in ion-channel based biosensors [193]. In some examples, two-dimensional transport is achieved either by diffusion, spreading [194], electric field [195], thermophoresis [Gözen et al, unpublished], hydrodynamic shearing [196] or surface acoustic waves [197]. Others use biomembranes as a natural medium for handling membrane proteins, including their accumulation [198] and separation [196]. In some cases, supported membrane are used for bulk coating, while in other instances micropatterns are needed. The lipid membrane can be patterned with the assistance of surface structures [194, 199], or lithographically, using soft-lithographic stamping [200], DPN [201] or even by microfluidic flow chambers [202]. Paper VII presents a novel concept of using a HCF of small unilamellar vesicles as a means to pattern compositionally diverse membrane circuits.



SUMMARY

This work describes the development of microfluidic technology for spatial and temporal manipulation of chemical microenvironments at the size scale of a single cell.

In **Paper I** a microfluidic dilution system is presented. The dilution is based on pulse width flow modulation (PWFM), where fluid streams are multiplexed using pneumatically actuated microvalves made in PDMS. By balancing the accuracy of the shortest pulse lengths and response time, we found that up to 10-fold dilution per stage and about 5s response time are feasible. In order to achieve a wider range of dilutions, multiple stages can be combined in series (two in this paper and three in a follow up-study). Since PDMS channels deform under pressure, which causes non-linear resistance and compliance effects, the circuits were made to maintain, ideally, the same pressure and flow in every switching state. The main features and advantages of this diluter are the low-cost PDMS fabrication, fast response time, time-dependent output through a single channel, continuously variable concentration settings, a minimal number of control channels (serial control signal), and a simple control system, where no pressure regulation is needed, only digital valves. Some drawbacks are the required calibration and the limited dynamic range. In the paper the diluter was characterized using fluorescence and electrochemical measurements, and finally applied to control the spreading of supported lipid-double bilayers. In a follow up study, which is not included in this thesis, a three stage diluter was fabricated, and a fully automated calibration and deployment system was developed [*Gemmer, Ainla and Jesorka*]. This diluter was eventually modified to allow liquid exchange in front of its outlet. This gave rise to the concept of the microfluidic pipette.

Paper II introduces the microfluidic pipette. Compared to the diluter shown in paper I, which also features an open volume outlet, the channel exits are here concentrated in the sharp tip of the device. This allows to position them next to objects of interest on a surface, i.e., it is a free standing device. Another aspect is the simultaneously applied inflow, which allows the outflowing liquid to be confined in a small volume - a hydrodynamically confined flow (HCF). In this paper the properties of the HCF were studied and the device was combined with a simple one-stage PWFM diluter, which

used a valveless switching principle based on hydrodynamic flow steering. The microfluidic pipette was used in several single-cell applications, to induce membrane zeiosis (blebbing), stimulate ion-channels in electrophysiology experiments, and to perform dose-response measurements.

Paper III describes the reshaping of the initial pipette prototype into a real multifunctional research tool. Practical inconveniences associated with its use were removed. Most importantly, shape and interfacing were improved, adjusting the device to the environment of biological microscopy, which is, typically, crowded by the objective, condenser lens, dish edge and other needles and probes. Therefore, a narrow and elongated design with a sharp tip has been chosen. Another important aspect was efficient interfacing, which is required to facilitate quick set-up, to prevent leaks and contamination and to reduce cleaning needs. This has been achieved by using integrated wells, which preserve solutions and have no dead volumes to fill. Since the simple, low-cost pipette tip can be considered to be disposable, there is also no need for cleaning and no risk of contamination. The first presented function of this new pipette was fast switching between three solution environments, which yielded about 200 ms exchange time. The switching process and the contributing factors were analyzed theoretically, and by means of computational models. This theoretical insight has been used later (Xu et al. unpublished manuscript and Paper VI & VII) to further improve the circuitry, now being capable of switching between four solutions in 50-100 ms. Further improvements and novel functions are easy to introduce, due to the modularity of the design. New circuits are integrated at the cost and effort of fabricating a channel structure on a silicon wafer - the molding tools as well as the holders are reused without modifications. The efforts were rewarded by the editors of Lab on a Chip, who elected our technology into the top 10% technologies!

Paper IV extends the capabilities of the multifunctional pipette by integrating electrodes into the PDMS device. It is difficult to use conventional metal patterning techniques on PDMS, owed to the poor adhesion between the materials. Therefore, our approach was to fill the channels with the low-melting Field's metal. This method is favorable, as high conductivity electrodes can be post processed by means of a simple hot-plate and a pump. The modified pipettes were used to combine localized solution delivery and electroporation of single adherent cells. A shortcoming of this approach is the brittleness of Field's metal structures. The otherwise robust tip became fragile and sensitive to bending. More flexible future alternatives could involve conductive polymer composites, but they exhibit lower conductivity and require larger channels, as the materials are more viscous and coarse.

Paper V explores applications of the pipette on rat brain slices. As discussed already in previous chapter, neuroscience is in great need for fast superfusion, while the high

spatial organization of the brain requires confined stimulation. Microfluidics is generally well suited for these tasks, but harder to apply in tissues. Specific chambers to hold tissue in the device are required [203]. The pipette provides an easier alternative, allowing electrophysiological experiments to be performed in their conventional environments (e.g. oxygenation). A distinct benefit of the pipette is faster solution exchange time compared to the conventionally used whole-slice perfusion. Localized stimulation not only allows new types of experiments to be performed, it also aids in the economic use of resources, as more data sets per slice can be collected, increasing efficiency and saving the lives of animals.

In **Paper VI**, the advantages of solution exchange and confinement are harnessed in a fluorescence based optofluidic thermometer, where the HCF allows contamination-free delivery of dyes, used for direct temperature measurement in the physiological temperature range. Switching between two fluorophores of different temperature dependent fluorescence intensity is used to create a reference system capable of eliminating microscope and alignment specific variability. This measurement technique was used together with a fiber optic microheater, to observe heat activation of temperature sensitive ion-channel (*hTRPV1*), monitored as an uptake of YO-PRO-1 to the channels.

Finally, **Paper VII** is engaging the pipette to implement a unique rapid prototyping platform for 2D nanofluidic circuits based upon supported lipid bilayers. The lipid material is locally deposited from small unilamellar vesicles, which are fusing into a continuous membrane, where molecules can be transported by diffusion and, in some cases, by capillary or shear forces. The geometry and composition of the circuitry is defined by synchronous computer controlled switching between membrane sources and scanning of the microscope stage. In addition to writing such compositionally diverse networks, they can be at any point removed, repaired or functionalized in a single experiment. This large variety of possibilities to manipulate lipid films and attached compounds constitutes a **lab on a membrane**, useful to controllably and conveniently study transport of membrane components and their interactions.

Conclusion and remarks

My research described in this thesis has been focused on the development of a microfluidic liquid handling tool, starting from basic principles and finishing with a refined instrument, which has been diversely applied in studies on cell cultures, tissue slices and biomimetic membranes. Locally controlled liquid handling can also be the foundation for other independent techniques, such as microthermometry and most notably: the writing of two-dimensional nanofluidic networks.

All the functions presented here are based on the concept of localized solution exchange. This is, however, just one possible aspect of the use of this device. Perhaps more desirable, but also more challenging is the opposite: collection and analysis of cellular content or release. Proteins are expressed in really tiny quantities: amounts in the 200 zmol range are typical according to [204], which correspond to just 100'000 molecules. Many rare proteins are even less abundant.

Another exciting area for future studies is the *Lab on a Membrane* and its applications in investigations of molecules confined in 2D liquids. On one hand, direct analysis of membrane proteins and their behavior is central to fundamental understanding of cell biology and aids in the development of new drugs. On the another hand, 2D fluidity represents a fundamentally different transport mode and a special environment for chemistry. Simplicity and robustness of our method may render 2D chemistry practically useable. Particularly fascinating is the combination of 2D fluidic and 2D electronics. One can envision connecting molecularly thin flows and graphene sensors to create new analytical techniques, able to detect just a few molecules extracted from a single cell. Even if the multifunctional pipette will be not an active part of membrane based detection devices, it may become a development tool as indispensable as the oscilloscope is for the development of electronics.

I believe that this technology, being functional, robust and simple to use, will find its way into many bioscience labs. It will enable new kinds of experiments, will improve data quality and ensure the efficient use of reagents, cell cultures and tissues. But after all, most of the exciting journey is still ahead of us: to discover new applications and abilities and solve questions and problems which we, at this point, are not even aware of.



ACKNOWLEDGEMENTS

These past five years, when I have been working on my PhD, have been the greatest fun! And the biggest contributors to this joy are, you, wonderful people, from all over the world, whom I have had opportunity to meet here, work together, gain ideas and inspiration, share struggles, excitement and celebrate successes, both between the lab walls and during free times! You have made it a memorable journey of my life!

Thanks ...

Owe: for accepting me as a PhD student in your lab and for believing in my work and the choices and for your vision and motivating passion towards the research.

Aldo: for being the best mentor, colleague and friend, a great scientist, who is always filled with curiosity and limitless enthusiasm to try even the wildest ideas! For always being helpful and opened to share your diverse knowledge and expertise - these thousands of hours of discussions about science, technology and philosophy has taught me a lot and also brought up many interesting ideas! Not to mention your immense contribution to all these developments and writing our papers, but also for proof reading my thesis, suggestions and improvements.

My co-authors:

Gavin: for all the work which we have done together to develop the pipette, most of all, for your mastery of design and fine mechanics, which has given our pipette its elegant shape and look. And for always rescuing us, when we got into trouble with optics and microscopes, as well as with challenges in English grammar. Not less important, for all the coffee-corner discussions, which although killed a bit of time, were always keeping me updated about the latest and coolest tech news!

Irep: for skipping the last trams and sleeping time, to sit after midnight in the confocal lab and pursue both our coolest (the very first tests of the pipette and the lab on a membrane) and sometimes most challenging experiments - that's the spirit! For keeping up enthusiasm and positive attitude, but also for the other fun outside of the confocal lab! ...and for all the help in this final thesis rush!

Kent: for the introduction to the interesting field of neuroscience, and rats and brains and electrophysiology. For being such a great host and having good times in Stockholm and at Karolinska.

Erik: for being able to watch over your shoulder, and learn about all the struggles and 'black magic' of patch-clamp. And of course, for your great company in all the conferences and being my Trans-Atlantic Swedish teacher!

Natasha: For handling cell blebbis and being a good snowboard teacher.

Also **Ilona, Bodil, Shijun, Aikram, Ralf, Holger & Nicolas** - for your great contributions to make all these different developments and experiments possible.

Our young, enthusiastic and driven microfluidics team, featuring:

Anna, Kiryl, Anil, Davood & Fredrik: for all the new ideas and for trying them out to bring about the next generations of devices! A pity that lately, in my thesis rush, I haven't had enough time to discuss with you, as much as I wish I would have.

OrwarLab:

For creating a nice, friendly, cooperative and warm atmosphere, that coming to the lab is almost like coming home. For our present (**Mehrnaz, Celine, Carolina, Haijiang**) & former (**Brigitte, Maria, Ilja, Johan, Tanya, Helen, Ludvig, Martin, Jian, Jessica, Lidiya, Inga**) members.

Andreas for taking the challenge of further developing the microfluidic diluter. **Paul** for your great knowledge and compelling discussions about different field of sciences.

The Collectricon team:

Christer, Fredrik, Glenn & Mattias for sharing your expertise and helping us to develop the production of high-quality pipettes, which have allowed us to do a large part of the research presented here. Big thanks also to the **Chalmers NanoInitiative**, whose financial support made this collaboration possible.

Collaborators & contributors:

Jelena, Carina, Ann-Sofie, Andy (Chalmers/GU), **Joseph Bruton** and **Håkan Westerblad** (Karolinska Institute), **Claudio Rivera** (University of Helsinki), **Olivier Curet** (Sanofi, Paris): for teaching me some new techniques, contributing to experiments, having interesting discussions, shearing insight into your exciting research and testing our devices in your projects. I have learned a lot!

The MC2 crew: **John, Johan, Hendrik, Ulf, Göran**: for teaching and helping with all the cleanroom machines.

My other friends:

Beer Club members: you made my Thursdays! Fortunately you were far too many (98!) to be listed here. But one of the spirits of the BC has been, of course, **Michal** - who besides other fun, is a master of delicious smoked fishes and bbq's.

Important people on the way, without whom I wouldn't be here: my high-school teacher **Ene**, who inspired me to study physics; my mentor in Estonia, **Alvo**, who inspired me to work in science; my friend **Triinu**, from whom I heard about Chalmers; **Alfred Ots' Scholarship Foundation**, which made my MSc. studies here possible; **Göran Wendin & Zoran**, thank to whom I met Aldo, and rest you already know ...

All my friends from all over the world!

My Estonian friends both here in Sweden and in Estonia! Especially **Mart**, the greatest friend of all Estonian Chalmers students, for your cheerfulness and care in arranging the delightful series of student symposia and many memorable dinners.

Annemarie: for the experience to have cats, and wonderful midsummers.

Our International Hiking Team: **Ludo, Toma, Masha, Gaizka**: for the reason to wait for the summers and the next adventures!

Vika: For many-many nice times together, great hikes and explorations, patience, kindness, support and good spirit toward science.

My family: **Mom, Dad & Tanel**: for unconditional love and support for all my endeavors. At first, for home, guidance and environment, where my young scientific curiosity has been nourished (including the sacrifice of numerous domestic gadgets). Later always encouraging my educational and scientific pursuits. Tanel: also for his advices and help in technology development. *Kallid Mammi ja Papi! Suur aitähh kõige eest ja vabandused, kui mul viimastel aegadel nii vähe aega on olnud, aga nüüd on see siis tehtud!*

Tack så Mycket! Suur Aitähh! Big Thanks!

REFERENCES

1. Tricorder. Wikipedia. (<http://en.wikipedia.org/wiki/Tricorder>)
2. Terry SC, Jerman JH, & Angell JB (1979) GAS-CHROMATOGRAPHIC AIR ANALYZER FABRICATED ON A SILICON-WAFER. *IEEE Transactions on Electron Devices* 26(12):1880-1886.
3. Karlsson R, Michaelsson A, & Mattsson L (1991) KINETIC-ANALYSIS OF MONOCLONAL ANTIBODY-ANTIGEN INTERACTIONS WITH A NEW BIOSENSOR BASED ANALYTICAL SYSTEM. *Journal of Immunological Methods* 145(1-2):229-240.
4. Becker H (2009) Hype, hope and hubris: the quest for the killer application in microfluidics. *Lab Chip* 9(15):2119-2122.
5. Chin CD, Linder V, & Sia SK (2012) Commercialization of microfluidic point-of-care diagnostic devices. *Lab Chip* 12(12):2118-2134.
6. Waters H (2011) New \$10 million X Prize launched for tricorder-style medical device. *Nat Med* 17(7):754-754.
7. Moore GA (1991) *Crossing the Chasm* (Harper Business Essentials).
8. Rogers EM (1962) *Diffusion of innovations* (Free Press., New York).
9. Existence and Smoothness of the Navier-Stokes Equation. Clay Mathematics Institute. (http://www.claymath.org/millennium/Navier-Stokes_Equations/)
10. Bruus H (2007) *Theoretical Microfluidics* (Oxford University Press).
11. Jeon NL, *et al.* (2002) Neutrophil chemotaxis in linear and complex gradients of interleukin-8 formed in a microfabricated device. *Nat Biotechnol.* 20(8):826-830.
12. Weigl BH & Yager P (1999) Microfluidics - Microfluidic diffusion-based separation and detection. *Science* 283(5400):346-347.
13. Yung CW, Fiering J, Mueller AJ, & Ingber DE (2009) Micromagnetic-microfluidic blood cleansing device. *Lab Chip* 9(9):1171-1177.
14. Cho BS, *et al.* (2003) Passively driven integrated microfluidic system for separation of motile sperm. *Analytical Chemistry* 75(7):1671-1675.
15. Probstein RF (2003) *Physiochemical Hydrodynamics* (Wiley-Interscience).
16. Taylor G (1953) DISPERSION OF SOLUBLE MATTER IN SOLVENT FLOWING SLOWLY THROUGH A TUBE. *Proceedings of the Royal Society of London Series a-Mathematical and Physical Sciences* 219(1137):186-203.
17. Aris R (1956) ON THE DISPERSION OF A SOLUTE IN A FLUID FLOWING THROUGH A TUBE. *Proceedings of the Royal Society of London Series a-Mathematical and Physical Sciences* 235(1200):67-77.

18. Azizi F & Mastrangelo CH (2008) Generation of dynamic chemical signals with pulse code modulators. *Lab Chip* 8(6):907-912.
19. Lucchetta EM, Lee JH, Fu LA, Patel NH, & Ismagilov RF (2005) Dynamics of Drosophila embryonic patterning network perturbed in space and time using microfluidics. *Nature* 434(7037):1134-1138.
20. Mosadegh B, *et al.* (2010) Integrated elastomeric components for autonomous regulation of sequential and oscillatory flow switching in microfluidic devices. *Nature Physics* 6(6):433-437.
21. Nguyen TV, Duncan PN, Ahrar S, & Hui EE (2012) Semi-autonomous liquid handling via on-chip pneumatic digital logic. *Lab Chip* 12(20):3991-3994.
22. Rhee M & Burns MA (2009) Microfluidic pneumatic logic circuits and digital pneumatic microprocessors for integrated microfluidic systems. *Lab Chip* 9(21):3131-3143.
23. Langelier SM, *et al.* (2011) Flexible casting of modular self-aligning microfluidic assembly blocks. *Lab Chip* 11(9):1679-1687.
24. Yuen PK (2008) SmartBuild - A truly plug-n-play modular microfluidic system. *Lab Chip* 8(8):1374-1378.
25. Duffy DC, McDonald JC, Schueller OJA, & Whitesides GM (1998) Rapid prototyping of microfluidic systems in poly(dimethylsiloxane). *Analytical Chemistry* 70(23):4974-4984.
26. Becker H, Beckert E, & Gartner C (2010) Hybrid tooling technologies for injection molded and hot embossed polymeric microfluidic devices. *Microfluidics, Biomems, and Medical Microsystems Viii*, Proceedings of SPIE, eds Becker H & Wang W (Spie-Int Soc Optical Engineering, Bellingham), Vol 7593.
27. Liao Y, *et al.* (2012) Rapid prototyping of three-dimensional microfluidic mixers in glass by femtosecond laser direct writing. *Lab Chip* 12(4):746-749.
28. Agirregabiria M, *et al.* (2005) Fabrication of SU-8 multilayer microstructures based on successive CMOS compatible adhesive bonding and releasing steps. *Lab Chip* 5(5):545-552.
29. Hull CW (1984) US 4,575,330.
30. THE FORM 1. 3D PRINTER. FormLabs. (<http://formlabs.com>)
31. Choi J-W, MacDonald E, & Wicker R (2010) Multi-material microstereolithography. *International Journal of Advanced Manufacturing Technology* 49(5-8):543-551.
32. LaFratta CN, Fourkas JT, Baldacchini T, & Farrer RA (2007) Multiphoton fabrication. *Angew Chem Int Edit* 46(33):6238-6258.
33. Murphy SV, Skardal A, & Atala A (2013) Evaluation of hydrogels for bio-printing applications. *J. Biomed. Mater. Res. Part A* 101A(1):272-284.

34. Xu T, *et al.* (2013) Complex heterogeneous tissue constructs containing multiple cell types prepared by inkjet printing technology. *Biomaterials* 34(1):130-139.
35. Symes MD, *et al.* (2012) Integrated 3D-printed reactionware for chemical synthesis and analysis. *Nat. Chem.* 4(5):349-354.
36. Kitson PJ, Rosnes MH, Sans V, Dragone V, & Cronin L (2012) Configurable 3D-Printed millifluidic and microfluidic 'lab on a chip' reactionware devices. *Lab Chip* 12(18):3267-3271.
37. (2012) Manufacturing. The third industrial revolution *The Economist*
38. Madou MJ (2002) *Fundamentals of Microfabrication. The Science of Miniaturization. 2nd Ed.* (CRC Press).
39. Iliescu C, Taylor H, Avram M, Miao J, & Franssila S (2012) A practical guide for the fabrication of microfluidic devices using glass and silicon. *Biomicrofluidics* 6(1).
40. Bu MQ, Melvin T, Ensell GJ, Wilkinson JS, & Evans AGR (2004) A new masking technology for deep glass etching and its microfluidic application. *Sens. Actuator A-Phys.* 115(2-3):476-482.
41. Laermer F & Schilp A (WO9414187-A; DE4241045-C; EP625285-A; DE4241045-C2; DE4241045-A1; DE4241045-C1; WO9414187-A1; EP625285-A1; JP7503815-W; US5501893-A; EP625285-B1; JP2007129260-A; JP4090492-B2).
42. Richter K, Orfert M, Howitz S, & Thierbach S (1999) Deep plasma silicon etch for microfluidic applications. *Surf. Coat. Technol.* 116:461-467.
43. SOI Wafers. Virginia Semiconductor Inc. (<http://www.virginiasemi.com>)
44. Pihl J, *et al.* (2005) Microfluidic gradient-generating device for pharmacological profiling. *Analytical Chemistry* 77(13):3897-3903.
45. Akashi T & Yoshimura Y (2008) Profile control of a borosilicate-glass groove formed by deep reactive ion etching. *Journal of Micromechanics and Microengineering* 18(10).
46. Malek CGK (2006) Laser processing for bio-microfluidics applications (part I). *Analytical and Bioanalytical Chemistry* 385(8):1351-1361.
47. Malek CGK (2006) Laser processing for bio-microfluidics applications (part II). *Analytical and Bioanalytical Chemistry* 385(8):1362-1369.
48. Chung CK, *et al.* (2010) Water-assisted CO₂ laser ablated glass and modified thermal bonding for capillary-driven bio-fluidic application. *Biomedical Microdevices* 12(1):107-114.
49. Huft J, Da Costa DJ, Walker D, & Hansen CL (2010) Three-dimensional large-scale microfluidic integration by laser ablation of interlayer connections. *Lab Chip* 10(18):2358-2365.

50. Becker H & Gaertner C (2008) Polymer microfabrication technologies for microfluidic systems. *Analytical and Bioanalytical Chemistry* 390(1):89-111.
51. Hupert ML, et al. (2007) Evaluation of micromilled metal mold masters for the replication of microchip electrophoresis devices. *Microfluid. Nanofluid.* 3(1):1-11.
52. Hupert ML, et al. (2006) High-precision micromilling for low-cost fabrication of metal mold masters - art. no. 61120B. *Microfluidics, BioMEMS, and Medical Microsystems IV*, Proceedings of the Society of Photo-Optical Instrumentation Engineers (Spie), eds Papautsky I & Wang W (Spie-Int Soc Optical Engineering, Bellingham), Vol 6112, pp B1120-B1120.
53. Schaller T, Bohn L, Mayer J, & Schubert K (1999) Microstructure grooves with a width of less than 50 μ m cut with ground hard metal micro end mills. *Precis. Eng.-J. Am. Soc. Precis. Eng.* 23(4):229-235.
54. Micron mills. Performance Microtools. (<http://www.pmtnow.com/>)
55. Iida K, et al. (2009) Living anionic polymerization using a microfluidic reactor. *Lab Chip* 9(2):339-345.
56. Lin YS, et al. (2012) An Aluminum Microfluidic Chip Fabrication Using a Convenient Micromilling Process for Fluorescent Poly(DL-lactide-co-glycolide) Microparticle Generation. *Sensors* 12(2):1455-1467.
57. Becker H & Gartner C (2000) Polymer microfabrication methods for microfluidic analytical applications. *Electrophoresis* 21(1):12-26.
58. Attia UM, Marson S, & Alcock JR (2009) Micro-injection moulding of polymer microfluidic devices. *Microfluid. Nanofluid.* 7(1):1-28.
59. Heckele M & Schomburg WK (2004) Review on micro molding of thermoplastic polymers. *Journal of Micromechanics and Microengineering* 14(3):R1-R14.
60. Becker H & Heim U (1999) Polymer hot embossing with silicon master structures. *Sens. Mater.* 11(5):297-304.
61. Anwar K, Han T, & Kim SM (2011) Reversible sealing techniques for microdevice applications. *Sensors and Actuators B-Chemical* 153(2):301-311.
62. Rhee SW, et al. (2005) Patterned cell culture inside microfluidic devices. *Lab Chip* 5(1):102-107.
63. Heidelberg Instruments. (<http://www.himt.de>)
64. Satyanarayana S, Karnik RN, & Majumdar A (2005) Stamp-and-stick room-temperature bonding technique for microdevices. *Journal of Microelectromechanical Systems* 14(2):392-399.
65. Kim K, Park SW, & Yang SS (2010) The optimization of PDMS-PMMA bonding process using silane primer. *BioChip.J.* 4(2):148-154.

66. Sunkara V, Park DK, & Cho YK (2012) Versatile method for bonding hard and soft materials. *RSC Adv.* 2(24):9066-9070.
67. Temnico YH, Koesdjojo MT, Kondo S, Mandrell DT, & Remcho VT (2010) Surface modification-assisted bonding of polymer-based microfluidic devices. *Sensors and Actuators B-Chemical* 143(2):799-804.
68. Bhattacharyya A & Klapperich CM (2006) Thermoplastic microfluidic device for on-chip purification of nucleic acids for disposable diagnostics. *Analytical Chemistry* 78(3):788-792.
69. Tsao CW & DeVoe DL (2009) Bonding of thermoplastic polymer microfluidics. *Microfluid. Nanofluid.* 6(1):1-16.
70. Brown L, Koerner T, Horton JH, & Oleschuk RD (2006) Fabrication and characterization of poly(methylmethacrylate) microfluidic devices bonded using surface modifications and solvents. *Lab Chip* 6(1):66-73.
71. Wei J, Xie H, Nai ML, Wong CK, & Lee LC (2003) Low temperature wafer anodic bonding. *Journal of Micromechanics and Microengineering* 13(2):217-222.
72. Allen PB & Chiu DT (2008) Calcium-assisted glass-to-glass bonding for fabrication of glass microfluidic devices. *Analytical Chemistry* 80(18):7153-7157.
73. Martinez AW, Phillips ST, Whitesides GM, & Carrilho E (2010) Diagnostics for the Developing World: Microfluidic Paper-Based Analytical Devices. *Analytical Chemistry* 82(1):3-10.
74. Li X, Tian JF, & Shen W (2010) Thread as a Versatile Material for Low-Cost Microfluidic Diagnostics. *ACS Appl. Mater. Interfaces* 2(1):1-6.
75. Safavieh R, Zhou GZ, & Juncker D (2011) Microfluidics made of yarns and knots: from fundamental properties to simple networks and operations. *Lab Chip* 11(15):2618-2624.
76. Foturan Photosensitive Glass. Invenios. (<http://www.invenios.com/>)
77. Bruin GJM (2000) Recent developments in electrokinetically driven analysis on microfabricated devices. *Electrophoresis* 21(18):3931-3951.
78. Mellors JS, Gorbounov V, Ramsey RS, & Ramsey JM (2008) Fully integrated glass microfluidic device for performing high-efficiency capillary electrophoresis and electrospray ionization mass spectrometry. *Analytical Chemistry* 80(18):6881-6887.
79. Fiorini GS, Lorenz RM, Kuo JS, & Chiu DT (2004) Rapid prototyping of thermoset polyester microfluidic devices. *Analytical Chemistry* 76(16):4697-4704.
80. Metz S, Holzer R, & Renaud P (2001) Polyimide-based microfluidic devices. *Lab Chip* 1(1):29-34.

81. Unger MA, Chou HP, Thorsen T, Scherer A, & Quake SR (2000) Monolithic microfabricated valves and pumps by multilayer soft lithography. *Science* 288(5463):113-116.
82. Roy E, Geissler M, Galas JC, & Veres T (2011) Prototyping of microfluidic systems using a commercial thermoplastic elastomer. *Microfluid. Nanofluid.* 11(3):235-244.
83. Personal Communication with MC2 personal about costs of microfabrication.
84. The Photo-Mask Guide. JD Phototools. (<http://www.jdphoto.co.uk/>)
85. Gelorme JD, Cox RJ, & Gutierrez SAR (EP222187-A; JP62102242-A; BR8604549-A; US4882245-A; EP222187-B; DE3674340-G; ES2017615-B; CA1289803-C; JP95078628-B2).
86. SU-8 2000 Permanent Epoxy Resists. MicroChem Inc. (<http://www.microchem.com>)
87. Lecomte JP. Silicone in the Food Industries. Dow Corning. (<http://www.dowcorning.com/content/publishedlit/Chapter3.pdf>)
88. Xia YN & Whitesides GM (1998) Soft lithography. *Annual Review of Materials Science* 28:153-184.
89. Xia YN & Whitesides GM (1998) Soft lithography. *Angew Chem Int Edit* 37(5):551-575.
90. Lewis LN & Lewis N (1986) PLATINUM-CATALYZED HYDROSILYLATION - COLLOID FORMATION AS THE ESSENTIAL STEP. *J. Am. Chem. Soc.* 108(23):7228-7231.
91. Faglioni F, Blanco M, Goddard WA, & Saunders D (2002) Heterogeneous inhibition of homogeneous reactions: Karstedt catalyzed hydrosilylation. *J. Phys. Chem. B* 106(7):1714-1721.
92. Morin SA, et al. (2012) Camouflage and Display for Soft Machines. *Science* 337(6096):828-832.
93. Lee JN, Park C, & Whitesides GM (2003) Solvent compatibility of poly(dimethylsiloxane)-based microfluidic devices. *Analytical Chemistry* 75(23):6544-6554.
94. Jo BH, Van Lerberghe LM, Motsegood KM, & Beebe DJ (2000) Three-dimensional micro-channel fabrication in polydimethylsiloxane (PDMS) elastomer. *Journal of Microelectromechanical Systems* 9(1):76-81.
95. McDonald JC, et al. (2000) Fabrication of microfluidic systems in poly(dimethylsiloxane). *Electrophoresis* 21(1):27-40.
96. Rosenthal CK, et al. (2009) Milestones of Light Microscopy *Nature Milestones*
97. Hook R (1665) Micrographia: or Some Physiological Descriptions of Minute Bodies, Made by Magnifying Glasses with Observations and Inquiries

- Thereupon. (Project Gutenberg Literary Archive Foundation (<http://www.gutenberg.org>)).
98. Zernike F (1942) Phase contrast, a new method for the microscopic observation of transparent objects. *Physica* 9:686-698.
 99. Allen RD, David GB, & Nomarski G (1969) The zeiss-Nomarski differential interference equipment for transmitted-light microscopy. *Z Wiss Mikrosk* 69(4):193-221.
 100. Jablonski A (1933) Efficiency of anti-stokes fluorescence in dyes. *Nature* 131:839-840.
 101. Stokes GG (1852) On the Change of Refrangibility of Light. *Philosophical Transactions of the Royal Society of London* 142:463-562.
 102. Masters BR (2010) The Development of Fluorescence Microscopy. *ENCYCLOPEDIA OF LIFE SCIENCES*.
 103. Coons AH, Creech HJ, & Jones RN (1941) Immunological properties of an antibody containing a fluorescent group. *Proceedings of the Society for Experimental Biology and Medicine* 47(2):200-202.
 104. Magde D, Webb WW, & Elson E (1972) THERMODYNAMIC FLUCTUATIONS IN A REACTING SYSTEM - MEASUREMENT BY FLUORESCENCE CORRELATION SPECTROSCOPY. *Phys Rev Lett* 29(11):705-&.
 105. Peters R, Peters J, Tews KH, & Bahr W (1974) MICROFLUORIMETRIC STUDY OF TRANSLATIONAL DIFFUSION IN ERYTHROCYTE-MEMBRANES. *Biochim Biophys Acta* 367(3):282-294.
 106. Stryer L & Haugland RP (1967) ENERGY TRANSFER - A SPECTROSCOPIC RULER. *Proceedings of the National Academy of Sciences of the United States of America* 58(2):719-&.
 107. Denk W, Strickler JH, & Webb WW (1990) 2-PHOTON LASER SCANNING FLUORESCENCE MICROSCOPY. *Science* 248(4951):73-76.
 108. Martin MM & Lindqvist L (1975) PH-DEPENDENCE OF FLUORESCIN FLUORESCENCE. *Journal of Luminescence* 10(6):381-390.
 109. Rhodamine B. Sigma-Aldrich. (<http://www.sigmaaldrich.com>)
 110. Axelrod D (1981) CELL-SUBSTRATE CONTACTS ILLUMINATED BY TOTAL INTERNAL-REFLECTION FLUORESCENCE. *Journal of Cell Biology* 89(1):141-145.
 111. Total Internal Reflection Fluorescence (TIRF) Microscopy. Nikon. MicroscopyU. (<http://www.microscopyu.com/>)
 112. Minsky M (1957) US3013467.

113. Karstens T & Kobs K (1980) RHODAMINE-B AND RHODAMINE-101 AS REFERENCE SUBSTANCES FOR FLUORESCENCE QUANTUM YIELD MEASUREMENTS. *Journal of Physical Chemistry* 84(14):1871-1872.
114. Barilero T, Le Saux T, Gosse C, & Jullien L (2009) Fluorescent Thermometers for Dual-Emission-Wavelength Measurements: Molecular Engineering and Application to Thermal Imaging in a Microsystem. *Analytical Chemistry* 81(19):7988-8000.
115. Eberhard M & Erne P (1991) CALCIUM-BINDING TO FLUORESCENT CALCIUM INDICATORS - CALCIUM GREEN, CALCIUM ORANGE AND CALCIUM CRIMSON. *Biochemical and Biophysical Research Communications* 180(1):209-215.
116. Fluo-3 Calcium Indicator. Life Technologies. (<http://www.invitrogen.com>)
117. YO-PRO®-1 Iodide (491/509). Life Technologies. (<http://www.invitrogen.com>)
118. Nolkranz K, Farre C, Hurtig KJ, Rylander P, & Orwar O (2002) Functional screening of intracellular proteins in single cells and in patterned cell arrays using electroporation. *Analytical Chemistry* 74(16):4300-4305.
119. Prasher DC, Eckenrode VK, Ward WW, Prendergast FG, & Cormier MJ (1992) PRIMARY STRUCTURE OF THE AEQUOREA-VICTORIA GREEN-FLUORESCENT PROTEIN. *Gene* 111(2):229-233.
120. Thorlabs. (<http://www.thorlabs.com/>)
121. Dertinger SKW, Chiu DT, Jeon NL, & Whitesides GM (2001) Generation of gradients having complex shapes using microfluidic networks. *Analytical Chemistry* 73(6):1240-1246.
122. Bennett MR, et al. (2008) Metabolic gene regulation in a dynamically changing environment. *Nature* 454(7208):1119-1122.
123. Zhang X & Roper MG (2009) Microfluidic Perfusion System for Automated Delivery of Temporal Gradients to Islets of Langerhans. *Analytical Chemistry* 81(3):1162-1168.
124. Hansen CL, Sommer MOA, & Quake SR (2004) Systematic investigation of protein phase behavior with a microfluidic formulator. *Proceedings of the National Academy of Sciences of the United States of America* 101(40):14431-14436.
125. Paegel BM, Grover WH, Skelley AM, Mathies RA, & Joyce GF (2006) Microfluidic serial dilution circuit. *Analytical Chemistry* 78(21):7522-7527.
126. Hong JW, Chen Y, Anderson WF, & Quake SR (2006) Molecular biology on a microfluidic chip. *Journal of Physics-Condensed Matter* 18(18):S691-S701.
127. Chen RH & Cheng CM (2001) Study of spin coating properties of SU-8 thick-layer photoresist. *Advances in Resist Technology and Processing Xviii*,

- Pts 1 and 2*, Proceedings of the Society of Photo-Optical Instrumentation Engineers (Spie), ed Houlihan FM), Vol 4845, pp 494-501.
128. Iliescu C, Chen B, & Miao J (2008) On the wet etching of Pyrex glass. *Sens. Actuator A-Phys.* 143(1):154-161.
129. Miniature Electronic Pressure Controllers. Parker Precision Fluidics. (<http://www.parker.com>)
130. Yasui T, *et al.* (2011) Microfluidic baker's transformation device for three-dimensional rapid mixing. *Lab Chip* 11(19):3356-3360.
131. Nguyen NT & Wu ZG (2005) Micromixers - a review. *Journal of Micromechanics and Microengineering* 15(2):R1-R16.
132. Stroock AD, *et al.* (2002) Chaotic mixer for microchannels. *Science* 295(5555):647-651.
133. Ahmed D, Mao XL, Shi JJ, Juluri BK, & Huang TJ (2009) A millisecond micromixer via single-bubble-based acoustic streaming. *Lab Chip* 9(18):2738-2741.
134. Olofsson J, *et al.* (2005) A chemical waveform synthesizer. *Proceedings of the National Academy of Sciences of the United States of America* 102(23):8097-8102.
135. Gaddum JH (1961) PUSH-PULL CANNULAE. *Journal of Physiology-London* 155(1):P1-&.
136. Delgado JMR, Defeudis FV, Roth RH, Ryugo DK, & Mitruka BM (1972) DIALYTRODE FOR LONG-TERM INTRACEREBRAL PERfusion IN AWAKE MONKEYS. *Arch. Int. Pharmacodyn. Ther.* 198(1):9-&.
137. Kovacs DA, Zoll JG, & Erickson CK (1976) IMPROVED INTRACEREBRAL CHEMITRODE FOR CHEMICAL AND ELECTRICAL STUDIES OF BRAIN. *Pharmacol. Biochem. Behav.* 4(5):621-625.
138. Ungerste.U & Pycock C (1974) FUNCTIONAL CORRELATES OF DOPAMINE NEUROTRANSMISSION. *Bulletin Der Schweizerischen Akademie Der Medizinischen Wissenschaften* 30(1-3):44-55.
139. Elmquist WF & Sawchuk RJ (1997) Application of microdialysis in pharmacokinetic studies. *Pharm. Res.* 14(3):267-288.
140. Ungerstedt U (2009) Microdialysis in Neurointensive Care. ed 2nd (Stockholm).
141. Mitsumori K, *et al.* (JP11033506-A; US6230722-B1; US2001037819-A1; US6517635-B2; US42566-E.
142. Veselovsky NS, Engert F, & Lux HD (1996) Fast local superfusion technique. *Pflugers Archiv-European Journal of Physiology* 432(2):351-354.

143. Lohmann C, Finski A, & Bonhoeffer T (2005) Local calcium transients regulate the spontaneous motility of dendritic filopodia. *Nat. Neurosci.* 8(3):305-312.
144. Engert F & Bonhoeffer T (1997) Synapse specificity of long-term potentiation breaks down at short distances. *Nature* 388(6639):279-284.
145. Feinerman O & Moses E (2003) A picoliter 'fountain-pen' using co-axial dual pipettes. *J Neurosci Meth* 127(1):75-84.
146. Shiku H, *et al.* (2009) A microfluidic dual capillary probe to collect messenger RNA from adherent cells and spheroids. *Anal. Biochem.* 385(1):138-142.
147. Feinerman O, Rotem A, & Moses E (2008) Reliable neuronal logic devices from patterned hippocampal cultures. *Nature Physics* 4(12):967-973.
148. Feinerman O, Segal M, & Moses E (2005) Signal propagation along unidimensional neuronal networks. *J. Neurophysiol.* 94(5):3406-3416.
149. Klauke N, Smith GL, & Cooper JM (2007) Microfluidic partitioning of the extracellular space around single cardiac myocytes. *Analytical Chemistry* 79(3):1205-1212.
150. Juncker D, Schmid H, & Delamarche E (2005) Multipurpose microfluidic probe. *Nat. Mater.* 4(8):622-628.
151. Lovchik RD, Drechsler U, & Delamarche E (2009) Multilayered microfluidic probe heads. *Journal of Micromechanics and Microengineering* 19(11).
152. Kaigala GV, Lovchik RD, Drechsler U, & Delamarche E (2011) A Vertical Microfluidic Probe. *Langmuir* 27(9):5686-5698.
153. Queval A, *et al.* (2010) Chamber and microfluidic probe for microperfusion of organotypic brain slices. *Lab Chip* 10(3):326-334.
154. Lovchik RD, Kaigala GV, Georgiadis M, & Delamarche E (2012) Micro-immunohistochemistry using a microfluidic probe. *Lab Chip* 12(6):1040-1043.
155. Perrault CM, *et al.* (2010) Integrated microfluidic probe station. *Rev. Sci. Instrum.* 81(11).
156. Chen D, *et al.* (2008) The chemistrode: A droplet-based microfluidic device for stimulation and recording with high temporal, spatial, and chemical resolution. *Proceedings of the National Academy of Sciences of the United States of America* 105(44):16843-16848.
157. Chang-Yen DA, Myszka DG, & Gale BK (2006) A novel PDMS microfluidic spotter for fabrication of protein chips and microarrays. *Journal of Microelectromechanical Systems* 15(5):1145-1151.
158. Delamarche E, Juncker D, & Schmid H (2005) Microfluidics for processing surfaces and miniaturizing biological assays. *Adv. Mater.* 17(24):2911-2933.

159. Zhao B, Moore JS, & Beebe DJ (2001) Surface-directed liquid flow inside microchannels. *Science* 291(5506):1023-1026.
160. Momotenko D, Cortes-Salazar F, Lesch A, Wittstock G, & Girault HH (2011) Microfluidic Push-Pull Probe for Scanning Electrochemical Microscopy. *Analytical Chemistry* 83(13):5275-5282.
161. Cortes-Salazar F, Momotenko D, Girault HH, Lesch A, & Wittstock G (2011) Seeing Big with Scanning Electrochemical Microscopy. *Analytical Chemistry* 83(5):1493-1499.
162. Lodish H (2007) *Molecular Cell Biology* (Freeman & Co Ltd).
163. Buonomano DV (2007) The biology of time across different scales. *Nature Chemical Biology* 3(10):594-597.
164. Breitinger HG (2001) Fast kinetic analysis of ligand-gated ion channels. *Neuroscientist* 7(2):95-103.
165. Auzmendi J, Do Porto DF, Pallavicini C, & Moffatt L (2012) Achieving Maximal Speed of Solution Exchange for Patch Clamp Experiments. *PLoS One* 7(8).
166. Hamill OP, Marty A, Neher E, Sakmann B, & Sigworth FJ (1981) IMPROVED PATCH-CLAMP TECHNIQUES FOR HIGH-RESOLUTION CURRENT RECORDING FROM CELLS AND CELL-FREE MEMBRANE PATCHES. *Pflugers Archiv-European Journal of Physiology* 391(2):85-100.
167. Kakei M & Ashcroft FM (1987) A MICROFLOW SUPERFUSION SYSTEM FOR USE WITH EXCISED MEMBRANE PATCHES. *Pflugers Archiv-European Journal of Physiology* 409(3):337-341.
168. Maconochie DJ & Knight DE (1989) A METHOD FOR MAKING SOLUTION CHANGES IN THE SUB-MILLISECOND RANGE AT THE TIP OF A PATCH PIPETTE. *Pflugers Archiv-European Journal of Physiology* 414(5):589-596.
169. Sinclair J, et al. (2002) A cell-based bar code reader for high-throughput screening of ion channel-ligand interactions. *Analytical Chemistry* 74(24):6133-6138.
170. Hering S, Beech DJ, & Bolton TB (1987) A SIMPLE METHOD OF FAST EXTRACELLULAR SOLUTION EXCHANGE FOR THE STUDY OF WHOLE-CELL OR SINGLE CHANNEL CURRENTS USING PATCH-CLAMP TECHNIQUE. *Pflugers Archiv-European Journal of Physiology* 410(3):335-337.
171. Pidoplichko VI (1996) Dependence of solution exchange time on cell or patch linear dimensions in concentration jump experiments using patch-clamped sensory neurones. *Pflugers Archiv-European Journal of Physiology* 432(6):1074-1079.

172. Sachs F (1999) Practical limits on the maximal speed of solution exchange for patch clamp experiments. *Biophys. J.* 77(2):682-690.
173. Lu HP, Xun LY, & Xie XS (1998) Single-molecule enzymatic dynamics. *Science* 282(5395):1877-1882.
174. Zhuang XW, *et al.* (2000) A single-molecule study of RNA catalysis and folding. *Science* 288(5473):2048-+.
175. Losavio BE, Iyer V, Patel S, & Saggau P (2010) Acousto-optic laser scanning for multi-site photo-stimulation of single neurons in vitro. *J. Neural Eng.* 7(4).
176. Kramer RH, Fortin DL, & Trauner D (2009) New photochemical tools for controlling neuronal activity. *Curr. Opin. Neurobiol.* 19(5):544-552.
177. Herr NR, Belle AM, Daniel KB, Carelli RM, & Wightman RM (2010) Probing Presynaptic Regulation of Extracellular Dopamine with Iontophoresis. *ACS Chem. Neurosci.* 1(9):627-638.
178. Isaksson J, *et al.* (2007) Electronic control of Ca²⁺ signalling in neuronal cells using an organic electronic ion pump. *Nat. Mater.* 6(9):673-679.
179. Bruckbauer A, *et al.* (2007) Nanopipette delivery of individual molecules to cellular compartments for single-molecule fluorescence tracking. *Biophys. J.* 93(9):3120-3131.
180. Tavana H, *et al.* (2009) Nanolitre liquid patterning in aqueous environments for spatially defined reagent delivery to mammalian cells. *Nat. Mater.* 8(9):736-741.
181. Ginger DS, Zhang H, & Mirkin CA (2004) The evolution of dip-pen nanolithography. *Angew. Chem. Int. Ed.* 43(1):30-45.
182. Kim KH, Moldovan N, & Espinosa HD (2005) A nanofountain probe with sub-100 nm molecular writing resolution. *Small* 1(6):632-635.
183. Kim KH, *et al.* (2008) Direct delivery and submicrometer Patterning of DNA by a nanofountain probe. *Adv. Mater.* 20(2):330-+.
184. Meister A, *et al.* (2009) FluidFM: Combining Atomic Force Microscopy and Nanofluidics in a Universal Liquid Delivery System for Single Cell Applications and Beyond. *Nano Lett.* 9(6):2501-2507.
185. Lundstrom K (2006) Structural genomics for membrane proteins. *Cell. Mol. Life Sci.* 63(22):2597-2607.
186. Kapitza HG & Sackmann E (1980) LOCAL MEASUREMENT OF LATERAL MOTION IN ERYTHROCYTE-MEMBRANES BY PHOTOBLEACHING TECHNIQUE. *Biochim Biophys Acta* 595(1):56-64.
187. Bloom M, Evans E, & Mouritsen OG (1991) PHYSICAL-PROPERTIES OF THE FLUID LIPID-BILAYER COMPONENT OF CELL-MEMBRANES - A PERSPECTIVE. *Q. Rev. Biophys.* 24(3):293-397.

188. Israelachvili JN (2010) *Intermolecular and Surface Forces* (Academic Press).
189. Boal D (2001) *Mechanics of the Cell* (Cambridge University Press).
190. Abreu-Blanco MT, Verboon JM, & Parkhurst SM (2011) Cell wound repair in *Drosophila* occurs through three distinct phases of membrane and cytoskeletal remodeling. *Journal of Cell Biology* 193(3):455-464.
191. Castellana ET & Cremer PS (2006) Solid supported lipid bilayers: From biophysical studies to sensor design. *Surface Science Reports* 61(10):429-444.
192. Knoll W, *et al.* (2008) Solid supported lipid membranes: New concepts for the biomimetic functionalization of solid surfaces. *Biointerphases* 3(2):FA125-FA135.
193. Cornell BA, *et al.* (1997) A biosensor that uses ion-channel switches. *Nature* 387(6633):580-583.
194. Czolkos I, *et al.* (2009) Platform for Controlled Supramolecular Nanoassembly. *Nano Lett* 9(6):2482-2486.
195. Groves JT, Boxer SG, & McConnel HM (1997) Electric field-induced reorganization of two-component supported bilayer membranes. *Proceedings of the National Academy of Sciences of the United States of America* 94(25):13390-13395.
196. Jonsson P, Gunnarsson A, & Hook F (2011) Accumulation and Separation of Membrane-Bound Proteins Using Hydrodynamic Forces. *Analytical Chemistry* 83(2):604-611.
197. Hennig M, Neumann J, Wixforth A, Radler JO, & Schneider MF (2009) Dynamic patterns in a supported lipid bilayer driven by standing surface acoustic waves. *Lab Chip* 9(21):3050-3053.
198. Jonsson P, *et al.* (2012) Hydrodynamic trapping of molecules in lipid bilayers. *Proceedings of the National Academy of Sciences of the United States of America* 109(26):10328-10333.
199. Groves JT, Ulman N, & Boxer SG (1997) Micropatterning fluid lipid bilayers on solid supports. *Science* 275(5300):651-653.
200. Nafday OA, Lowry TW, & Lenhert S (2012) Multifunctional Lipid Multilayer Stamping. *Small* 8(7):1021-1028.
201. Lenhert S, *et al.* (2010) Lipid multilayer gratings. *Nat. Nanotechnol.* 5(4):275-279.
202. Smith KA, Gale BK, & Conboy JC (2008) Micropatterned Fluid Lipid Bilayer Arrays Created Using a Continuous Flow Microspotter. *Analytical Chemistry* 80(21):7980-7987.
203. Huang Y, Williams JC, & Johnson SM (2012) Brain slice on a chip: opportunities and challenges of applying microfluidic technology to intact tissues. *Lab Chip* 12(12):2103-2117.

204. Anselmetti D (2009) *Single Cell Analysis* (Wiley-VCH Verlag GmbH).